Satellite/Sensors for Monitoring Earth's Oceans from Space

ALFRED R. ZIEGER
G. CURTIS CLEVEN
EDGAR S. DAVIS
FRED S. SOLTIS
CRAIG L. PURDY, Goddard Space Flight Center

Jet Propulsion Laboratory
4800 Oak Grove Drive
Pasadena, CA91109-S099

Abstract *The TOPEX/Poseidon Satellite/Sensors compliment was designed to specifically measure the sea surface topography to an unprecedented precision of better than 14 cm. A brief description of the satellite and sensors accompanied by an operations overview provide a background for undemanding the mission. A brief presentation of systems and subsystems performance illustrates how the mission is substantially outperforming the overall performance requirements. More than one year of performance data are now available on which to bare these early results, This is very promising for the possibility* of *mission* lifetime achieving its 3-5 *year goals and beyond.*

Keywords TOPEX, Poseidon, satellite, sensors, altimeter, radiometer, GPS receiver, sea level

I. Introduction

To help celebrate the International Space Year, NASA and the French space agency, Centre National d'Etudes Spatiales (CNES), launched a satellite August 10, 1992 to measure the topography of the surface of the world's oceans. The Jet Propulsion Laboratory is managing the program for NASA. The satellite was launched aboard the French Ariane 42P launch vehicle from the Guiana Space Center in Kourou, French Guiana located on the northeast coast of South America. NASA Select television showed the night launch was very bright, the plume lit the pad area and sky as the rocket ascended into orbit. The location of the launch site and the path of the ground track are shown in Figure 1.0. The payload sensors were integrated into a spacecraft designed and built by Fairchild Space, under contract with the Jet Propulsion Laboratory.

The mission is primarily concerned with measuring the sea surface height from space which will enable scientists to determine ocean circulation and its effects on our environment. The transport of heat in the oceans affects the weather, global warming, rising sea level, and possibly other phenomena yet to be discovered. The satellite carries on-board radar altimeters that precisely measure the shallow hills and valleys of the ocean surface which are direct evidence of the circulation patterns of the oceans.

The satellite's 1336 km altitude and 66° inclination provides 90% global coverage. of the oceans. The 10 day repeating orbit provides about 36 data sets per year to help scientists study the oceans changes and explain the mysteries of the ocean's role in maintaining a habitable planet. This article briefly describes the satellite and sensors performance and their operations in support of the TOPEX/Poseidon Project. 'I'he. project development and operations schedule is included in Figure 2.0.

The primary mission will last for 3 years, the extended mission for an additional 2 years. The mission has been coordinated with a number of international oceanographic and meteorological programs, including the World Ocean Circulation Experiment (WOCE) and the Tropical Ocean and Global Atmosphere Programme (TOGA), both of which are sponsored by the World Climate Research Programme (WCRP). The observations of TOPEX/Poseidon are timed to provide a global perspective for interpreting the in situ measurements collected by these programs, which in turn will be combined with satellite observations to achieve a global description of the circulation of the world's oceans, In the autumn of 1987, an international team of 38 Principal Investigators was selected to participate in the mission, These scientists worked closely with the TOPEX/Poseidon Project in refining the mission design and science plans. They are now conducting a wide range of oceanographic and geophysical investigations using the TOPEX/Poseidon data to demonstrate the scientific utility of the mission to the international scientific community.

The primary scientific objective of the mission is a substantial increase in our understanding of global ocean dynamics by making precise and accurate observations of sea level for a minimum of 3 years. These observations will lead to the following: determination of the general circulation of the ocean and its variability; a test of the ability to compute circulation that results from forcing by winds; a description of the nature of ocean dynamics; calculation of the transport of heat, mass, nutrients, and salt by the oceans; determination of the geocentric ocean tides; an investigation of the interaction of currents with waves, The sea level observations will also make contributions to marine geophysics leading to improvement in the knowledge of the marine geoid and increased understanding of lithospheric and mantle processes.

11. Satellite/Sensors Overview and Background

A satellite altimeter system employs two techniques to arrive at sea level: radar altimetry and precision orbit determination. Radar altimetry is the precise measurement of the satellite's altitude above the ocean surface. Precision orbit determination is the measure of the' satellite's orbital distance from the center of the Earth. The difference between these two measurements is the height of the sea surface relative to the center of the Earth. This height is called sea level, which is the primary measurement of the mission, In addition to sea level, ocean wave height and wind speed can also be measured from the shape and strength, respectively, of the altimeter's return pulse.

The principal goal of TOPEX/POSEIDON is to measure sea level with unprecedented accuracy such that small amplitude, basin wide sea level changes caused by large-scale ocean circulation can be detected. To reach this goal, the sensor system and orbit for the mission have been optimally designed.

Satellite

The TOPEX/Poseidon satellite is an adaptation of the existing Fairchild Space Multi-Mission Modular Spacecraft (MMS), which has successfully carried the payloads of the Solar Maximum Mission in 1980, the Landsat-4 in 1982, the Landsat-5 in 1984. The MMS design was modified to meet the TOPEX/Poseidon requirements, The satellite bus consists of the MMS and the instrument Module. The Instrument Module houses all of the payload sensors, the solar array, the high gain antenna, and the instrument module interface unit. The satellite is continually pointing the altimeter antenna at the surface of the ocean under 3-axis control using reaction wheels, gyros, and celestial sensors.

The MMS houses the Command and Data Handling Subsystem, the onboard computer, three tape recorders, and electronics that provide control for all satellite engineering subsystems and sensors. The Attitude Determination and Control Subsystem, the star trackers, the Earth Sensor Assembly Module, and the Propulsion Module control attitude and orbit-adjust maneuvers throughout the mission. The Electrical Power Subsystem on the MMS provides power from the solar array and batteries to the satellite systems. The solar array is mounted to the Instrument Module, and its motion is controlled by the Solar Array Drive Assembly. The Radio Frequency Communications Subsystem includes the transmitters/receivers, the high-gain antenna, the two omni antennas, and provides forward- and return-link telecommunications capability through the Tracking and Data Relay Satellite System.

Sensors

There are six science instruments in the mission payload, four from NASA and two from CNES. They are divided into operational and experimental sensors as follows:

(1) Operational Sensors
   (a) Dual-Frequency Radar Altimeter (ALT) (NASA)
   (b) TOPEX Microwave Radiometer (TMR) (NASA)
   (c) Laser Retroreflector Array (LRA) (NASA)
   (d) Doppler Orbitography and Radio-positioning Integrated by Satellite. (DORIS) Dual-Doppler Tracking System Receiver (CNES)

(2) Experimental Sensors
   (a) Single-Frequency Solid-State Radar Altimeter (SSALT) (CNES)
   (b) Global Positioning System Demonstration Receiver (GPSDR) (NASA)

The ALT, operating at 13.6 GHz (Ku-band) and 5.3 GHz (C-band) simultaneously, is the primary instrument for the mission. The measurements made at the two frequencies

are combined to obtain precise. altimeter height measurements over the oceans of the. world, These two frequency measurements are corrected to first order for errors caused by ionospheric free electrons, of which the total electron content is obtained as a by-product of the measurement. This instrument is the first spaceborne altimeter that uses dual frequency measurements for ionospheric range corrections. The satellite configuration with locations for the satellite modules and instruments is shown in Figure 3.0.

The TMR uses the measurement of sea surface microwave brightness temperature at three frequencies (18 Ghz, 21 GHz, and 37 GHz) to estimate the total water-vapor content in the atmosphere along the beam of the altimeter; this estimate corrects path delay errors in the altimeter measurement that result from this source. The 21 GHz channel is the primary channel for water-vapor measurement. The 18 GHz and 37 GHz channels are used to remove the effects of wind speed and cloud cover, respectively, in the water-vapor measurement.

The LRA utilizes a global network of satellite laser ranging stations to provide the NASA baseline tracking data for precision orbit determination and calibration of the radar altimeter bias.

The DORIS tracking system provides the CNES baseline of tracking data using microwave doppler techniques for precision orbit determination. The DORIS system has been successfully demonstrated by the SPOT-2 Mission. The system is composed of an onboard receiver and a network of 40 to 50 ground transmitting stations providing all-weather global tracking of the satellite. The signals are transmitted at two frequencies (401,25 MHz and 2036.25 MHz) to allow removal of the effects of ionospheric free electrons in the tracking data. Therefore, the total content of the ionospheric free electrons can also be estimated from the DORIS data and used for the ionospheric correction for the SSALT.

The two experimental instruments are intended to demonstrate new technology. The GPSDR, operating at 1227.6 MHz and 1575.4 MHz, is part of a new technique based on the Global Positioning System (GPS) for precise, and continuous tracking of the spacecraft with better than decimeter accuracy. The SSALT, operating at a single frequency of 13.65 GHz, is validating the technology of a low-power and low-weight altimeter for future Earth observational missions. The SSALT shares the 1.5 m diameter antenna with the ALT; thus only one altimeter operates at any given time. The two altimeters share the large antenna to reduce weight and cost. Figure 4.0 presents a diagram of the fundamental measurements from the satellite and the geometry with the orbit and the ocean surface.

Orbit Determination

The. orbit enters into the measurement of sea level in two important ways. It dictates the temporal (time dependent) and spatial (distance dependent) sampling pattern of the

altimeter, which in turn dictates our ability to measure certain sea-surface features, In addition, because it supplies the reference for the altimeter measurement, the orbit enters directly into the computation of sea level; therefore, our "knowledge of the radial component of the orbit, as obtained through the process of orbit determination, is of great importance.

The inclination of the mission's orbit, which is 66.0 degrees, has been selected to avoid sampling the tidal signals at undesirable frequencies such as semiannual, annual, and zero frequencies (fixed biases), The precise sea-level measurements made by the altimeters can be used to improve the knowledge of tides and consequently to remove tides from the sea-level measurement, The orbit configuration has been optimized to avoid tidal aliasing at selectee] frequencies, hence, making certain that some tidal constituents are not mistaken for others. A repeat period of 10 days was selected as a compromise that takes temporal resolution, spatial resolution, and tidal aliasing into consideration. This choice results in an equatorial cross-track separation of 315 km. Hence, the final orbit is very nearly circular with an altitude of 1336 km at the equator crossing. Figure 5.0 shows the ground track of one 10 day cycle consisting of 127 orbits.

111. NASA Radar Altimeter

The NASA Radar Altimeter (NRA) is a downward looking radar system designed to measure the distance or range to the ocean surface directly below the satellite. Range is measured by timing the delay between transmitting a pulse of RF energy and receiving the echo reflected from the ocean surface, Other parameters such as significant wave height (SWH) and wind speed are inferred from the return pulse shape and amplitude. Figure 6.0 is a drawing of the altimeter system as represented for installation in the bottom portion of the TOPEX satellite. The aluminum honeycomb structure was provided by Fairchild Space for mounting of the altimeter subsystems, The NRA was designed fabricated and tested by the Applied Physics Laboratory/Johns Hopkins University under contract to NASA Goddard Space Flight Center, Wallops Flight Facility, Virginia.

The NRA design is based on the earlier SEASAT and GEOSAT altimeters. However, its design incorporates several changes from those altimeters to provide; a more precise height measurement, better accuracy, ionospheric path delay correction, and longer operational lifetime. The basic operating characteristics of the NRA are listed in Table 1.0. A simplified functional block diagram is given by Figure 7.0.

The dual-frequency approach is employed to derive and correct for path delay changes induced by electron content in the ionosphere. These corrections can be as much as 30 centimeters at the Ku-band frequency, Previous altimeters had to rely on less accurate ionospheric modeling for this correction. An ancillary result of this correction is the ability to produce global maps of ionosphere electron content. The altimeter has a pulse repetition frequency (PRF) at Ku-band of approximately 4220 pulses per second and

1220 pulses per second at C-band. It interleaves these transmissions and tracks their return simultaneously using the same receiver and signal processor. The higher PRFs allow for better precision particularly at higher significant wave heights,

In order to meet the required three year operational lifetime the altimeter is completely redundant at both frequencies except for the antenna and some passive components in the Microwave Transmission Unit. The redundant sides are designed for completely independent operation from each other. All interfaces with the satellite are independent for each side and cross strapped where possible,

The three-year life requirement combined with the predicted radiation environment required a stringent parts selection effort to utilize radiation tolerant parts where possible and provide metal shielding in some areas. It also required that the parts be non latch up sensitive and survive Single Event Upsets (SF. US) with the loss of a minimum amount of data. To assist in the last requirement a watchdog timer software routine was implemented to automatically detect and recover from most SEUs.

The altimeters processor design allows for reprogramability from the ground, The system may be completely reprogrammed or small portions of the program (modules) may be modified to either provide better operation or recover from emergency situations. A separate parameter select capability allows for easily changing many of the altimeters operating parameters (such as bandwidths, thresholds, etc.) via ground command. To date, the altimeter has undergone minor reprogramming to update certain parameters in memory and to help prevent data loss due to SEUS. Also the parameter select mode has been used many times to run tests, improve acquisition performance, and provide a more usable offset between the Ku and C-band height tracking capability.

Again, refer to Figure 7.0 the altimeter block diagram for the discussion below. The Altimeter's Low-Voltage Power Supply (LVPS) and Power Switching Unit (PSU) interface to the satellite power system. The LVPS supplies the voltages required by all parts of the altimeter system. The satellite bus 28 volts is supplied to the Traveling Wave Tube Amplifier (TWTA) and the C-Band Solid State Amplifier (CSSA) through relays in the PSU. All other voltages required within the altimeter are developed and conditioned within the LVPS.

The Up-Converter-Frequency Multiplier (UCFM) interfaces to the 5 MHz Frequency Reference Unit oscillator signal. From this input it develops the 125 MHz signal sent to the Chirp Generator (CG). The CG develops a chirped (linear frequency modulated) signal with a center frequency of 250 MHz and a chirp bandwidth of 80 MHz. This chirp signal is then routed back to the UCFM where it is multiplied up to a center frequency of 13.6 GHz for transmission and 13.1 GHz for the receiver Local Oscillator signal, both of these signals now have a chirp bandwidth of 320 MHz, The chirp bandwidth slopes from + 160 MHz to -160 MHz around the 13.6 GHz center frequency.

The UCFM also generates a frequency of 500 MHz which is used for the second down conversion within the receiver.

The Signal Switching Unit (SSU) then routes these signals to the transmitter, the receiver and the Down Converter Unit (DCU) where the equivalent C-band signals are developed. Likewise, the C-band chirp bandwidth is nominally 320 MHz similar to the Ku-band.

The Ku-band TWTA amplifies the 13.6 GHz chirp pulse to approximately 20 watts and routes it to the transmit path of the Ku-band Microwave Transmission Unit (MTU). The MTU monitors the power level and routes the signal to the antenna system for transmission towards the earth,

The C-band signal from the DCU is routed to the C-band Solid State Amplifier (CSSA) where it is amplified to approximately 20 watts and routed to the C-band MTU. In the MTU the peak power is monitored and the. C-band pulse is routed to the C-band port of the antenna for transmission to the ocean surface.

The antenna is a dual frequency parabolic antenna capable of handling both the Ku-band signal and the C-band signal simultaneously. It also has a second Ku-band port which handles the Ku-band signal transmission and reception from the French altimeter (SSALT). The two Ku-band ports are properly isolated via the use of an orthomode coupler which separately passes each frequency without significantly degrading the signals.

The Ku-band and the C-band signals are interspersed within a burst period, Within each transmitted burst there are 38 Ku-band pulses and 10 C-band pulses. The Ku pulses are transmitted during the C receive pulse period and vice versa, At the end of each burst is a variable time before transmission of the next burst. This time period is dependent on the actual height and is sufficient to cover the full range expected in flight. The burst method of transmission is required to obtain the high PRFs and dual frequency of operation without transmit and receive interference.

Upon reception of the reflected signals by the antenna; each frequency return is routed to its respective MTU where it is filtered, amplified, and de-ramped, This method allows retaining wide band (320 MHz) information within lower bandwidth IF signals that can be easily handled, This gives us an equivalent to a 32000 to 1 pulse compression ratio.

The 500 MHz signals from the de-ramping process are then routed to a common receiver where they undergo further filtering and gain control. After the signal amplitude is properly adjusted by the Automatic Gain Control (AGC) the signals are down converted to video Inphase and Quadrature (I&Q) components; These signals at both frequencies then feed to a common Digital Signal Processor unit (DSP).

A functional block diagram of the Digital Signal Processor is given in Figure 8.0. The received signals at each frequency are first sampled by the Digital Filter Bank where they are converted to 128 samples of power spectral data via a Fast Fourier Transform (FFT) algorithm. These samples are equivalent to the received signal in the frequency domain. This digitized wave form (at each frequency) is averaged over the tracker update interval (approximately 50 milliseconds) and then routed to the Adaptive Tracker Unit (ATU).

The ATU utilizes an Alpha-Beta tracking algorithm to track the leading edge of the return wave form. An Intel 80186 microprocessor is the heart of the ATU and runs the software which controls the altimeter. The height and critical data are updated every 6 bursts or about once every 50 ms. The ATU builds a frame of altimeter data every 20 update intervals or about once per second depending on the altitude. Each altimeter record includes 20 measurements each of Ku-band height, C-band height difference, Ku and C AGC voltage, and Ku and C significant wave height parameters. Each frame also includes 10 wave form samples of the primary frequency and 5 of the secondary frequency, normally Ku and C respectively.

The Synchronizer (SYNC) provides all clock and timing signals to the RF components, the DFB and the Interface Control Unit (ICU). The ICU interfaces the altimeter to the satellite bus. Telemetry and command functions are accomplished and metered through this unit.

The above discussion dealt with the normal tracking mode. The altimeter also has an internal calibration mode which allows for monitoring very precisely changes in altimeter height bias, overall loop gain, transmitted power, receiver noise characteristics and any changes within the wave form sampling system. It does this via two modes; Calibration 1 and Calibration 2. In mode 1 a chirp signal is generated then transmitted to the receiver chain through a very precise step attenuator, this signal is de-ramped and tracked by the signal processor. The step attenuator is stepped over a range of 32 dB in steps of 2 dB. At each step the loop is allowed to settle. Accurate height, AGC data and wave form sample data is recorded which allows monitoring changes in height bias, changes in overall loop gain transmitter performance and wave form sampler characteristics. In the Calibration 2 mode, the transmit signal is not routed to the receiver, instead the receiver looks at system noise and appropriately adjusts the system gain. This provides a look at system noise characteristics, receiver gain characteristics and wave form sampler performance.

ON-ORBIT PERFORMANCE

Height Noise:

The NRA is performing well within its requirement on the height noise measurement. Table 2.0 shows the on-orbit performance achieved versus the requirement for three different Significant Wave Heights (SWH). The performance is calculated on one second interval data. The calculation of the noise performance is done by a fairly quick

and easy method developed by G. S. Hayne and D. W. Hancock of NASA which relies on the theoretical relationships of the two frequencies to remove most geoidal effects. To help test this method, well defined test data was used to derive the same performance numbers that would have resulted from the much more rigorous processing. Figure 9,0 is a plot of height noise versus SWH derived via the same method.

Significant Wave Height:
Figure 10.0 is a histogram of SWH measurements (Ku-band only) for one complete cycle (10 days) of on-orbit data. It shows the same shape that we have seen in other radar altimeters and it peaks at the correct approximate value, that is about 2 meters. The SWH has also been checked against that derived by full waveform processing of the return signal and the results are identical. The Ku and C-band derived SWH agree with each other,

Normalized Radar Backscatter Coefficient (Sigma Zero):
This parameter, related to the back scatter energy level, is determined from the altimeter internal Automatic Gain Control (AGC) circuitry. This circuitry varies the overall receiver gain in order to keep the output of the receiver to the signal processor at a fixed level (it is actually a measure of inserted attenuation). As the return signal level goes up the AGC attenuation will increase in response. Figure 11.0 is a histogram of Sigma Zero for a full cycle of data. This histogram is the same shape as previous altimeters and peaks at the correct value for a worldwide average. Very good correlation between sigma zero and SWH has been achieved. This parameter is ultimately used to calculate the ocean surface windspeed in the sub satellite footprint.

Ionosphere Correction:
The effect of the ionospheric path delay is calculated by deriving a height measurement at Ku-band and C-band then combining the heights to derive the correction. Ionosphere delay is frequency dependent therefore with measurements made at two widely spaced frequencies. Figure 12.0 shows the Ionosphere Correction for 2 passes or one complete orbit. The data behaves as expected. The top pass is essentially the daytime portion of the orbit showing corrections as high as 12 cm with a double hump signature. The bottom pass is the “nighttime” part, showing, as expected, a very small effect from the ionosphere.

Height Bias Drift:
Drift in the height bias measurement is monitored in-flight by the internal calibration mode. Figure 13.0 shows the measured height difference from the reference height for one step of the calibration mode as compiled from turn on until the current date. From this data it can be seen that there has been no discernible drift in the height bias. The variations that look like spikes can be traced to calibration data when temperature changes occurred from satellite induced altimeter shutoffs.

Receiver Gain Changes:
Receiver gain changes are also monitored by the internal calibration mode. To date the only gain changes that are apparent appear to be in the calibration mode circuitry only and not in the normal path of the altimeter,

On-orbit difficulties;
Before launch it was calculated that for the given space environment that the NASA altimeter would experience about one SEU every 4 days, The watchdog timer software was included in the system design to help detect SEUs and automatically sequence the altimeter back to normal operation with a minimum of lost data. It was postulated that this timer would catch over 90% of all upsets. In the first 14 months of its operation the altimeter experienced 51 known upsets and automatically recovered from 4S of them. The upsets that have not been properly detected appear to be occurring in static registers that are not being dynamically updated. Since these upsets do not effect the track interval or burst interval times they are not detected by the "watchdog". A software patch could be developed to automatically refresh these registers on fixed intervals to prevent the loss of any amount of data, But, developing and testing this patch would involve some effort that currently has not been budgeted for. As an alternative new alarms have been implemented in the ground system at the mission operations control center that will alert the Flight Controller to such an occurrence whenever data is available (at least once per orbit). Recovery procedures have also been implemented in the ground system which should prevent the loss of any more than one orbits worth of data for any occurrence.

Because the data from the DFB has been looked at very extensively since launch in many different modes and conditions, several anomalies in this data have become apparent. These anomalies are basically excess signals which occur in some of the filter bins. They appear to be due to several different causes; mathematics of the Fast Fourier Transform., slight offsets in an Analog to Digital Converter, and low-level electromagnetic interference. Considerable effort has been expended in modeling these effects by G, S. Hayne and others (see Engineering Assessment Report, 9/93, in reference), Although, some of these conditions have a small effect on altimeter system performance, the ALT is still well within the requirements. Based on pre-launch test data, side B of the altimeter should exhibit less of these anomalies than side A does. Side B of the NRA has not yet been powered in orbit and will only be used if problems occur with side A. These anomalies were not readily apparent during ground testing due to the operating environment and limitations on the ground test hardware.

At both the Ku and C-band frequencies in certain ocean areas where the significant waveheight is very low, the AGC value rises fairly quickly by 6 dB or more. Along with this rise in AGC; the attitude correction Vatt calculation becomes more noisy, and the height noise increases. Vatt is a voltage measurement taken during ground testing that is proportional to off-nadir attitude angle. It appears that in these areas the return wave form departs from those predicted by the diffuse scattering model. The AGC system is

designed to work with the model return, departures from this model cause the AGC to operate differently than planned. Past altimeters have seen similar effects but because of the amount and precision of the TOPEX data they are more noticeable. It appears that less than 5% of the open deep ocean data exhibit these anomalies, in ground processing, data with these anomalies are flagged for the data user and will not be included in the GOOD DATA set,

At this point in time no other problem areas with the NASA Radar Altimeter have been identified. Its operation appears to be nominal with no signs of degradation or impending problems. All temperatures are well within the pre-flight predicted ranges, the transmitters appear to be operating nominally and all engineering parameters are stable and operating as designed.

IV, TOPEX Microwave Radiometer

Altitude accuracy as determined by the altimeter is affected by the variable water content of the atmosphere, mainly, the troposphere. The objective of the TOPEX Microwave Radiometer (TMR) is to measure the radiometric brightness temperature related to water vapor and liquid water in the same field-of-view as the altimeter. These brightness temperatures, in turn, are converted to path-delay information required by the altimeter for precise topography measurements,

The TMR provides a path delay correction for the radar altimeter with an accuracy of 1.2 cm or less over a 1-second period, which meets the TMR specification. The intrinsic residual in the path delay retrieval algorithm accounts for 0.8 cm of this error. This leaves an uncorrelated error budget of 0.9 cm for the TMR calibration. This is equivalent to a TMR calibration error budget of 1.1 K (degrees Kelvin). The brightness temperature antenna pattern correction and antenna temperature calibration algorithms have associated errors of 0.8 K and 0.65 K, respectively. This leaves an uncorrelated error budget of 0.4 K for the stochastic radiometer noise, or DELTA-T.

The TMR is composed primarily of an antenna, RF section, and digital section, see Figure 14.0. The TMR is attached externally to the instrument module and performs its own thermal control. A functional block diagram of the TMR is presented in Figure. 15.0. The diagram illustrates the functional relationships among the separate microwave radiometers and shows the manner in which they interconnect with, and are served by, a common collecting aperture. Path delay retrieval errors associated with the radiometer/altimeter footprint size and location differences have been incorporated into the 0.8-cm path delay intrinsic residual. A comparison of TMR parameters and functional requirements is shown in Table 3.0.

The TMR channels are identified in Table 4.0. The radiometer unit consists of four microwave receivers shown as channels R1 through R4. Each channel is of the conventional Dicke (switched) superheterodyne-type receiver as shown in Figure 16.0.

Table 4.0 TMR Channels Indicating Polarization and 21 GHz Redundancy

UNIT	CHANNEL AND POLARIZATION	FREQUENCY (GHZ)
Radiometers	R1 Horizontal	18
	R2 Horizontal	21
	R3 Vertical	21
	R4 Horizontal	37

The input to each channel is received from the multi-frequency feed horn at the off-set base of the antenna, Calibration of the radiometers is accomplished by alternatively switching to the sky calibration horns, viewing cold space (2.7 K), or to the warm (293 K) "base" load located inside the radiometer chassis. A calibration sequence is performed once during each major frame of TMR instrument data (28 seconds).

A two-position Dicke switch, switching at a rate of approximately 1kHz, compares the signal presented to its input with the ambient temperature "reference load." An isolator and low-noise mixer-preamp follow with a solid-state oscillator providing local oscillator power to the mixer. The mixer-preamp is followed by an Intermediate Frequency (IF) amplifier, video amplifier, phase detector and dc amplifier integrator which completes the channel. A logic signal from the programmer synchronizes the Dicke switch and phase detector. Also included in each radiometer channel are temperature sensors and various engineering monitor circuits.

The antenna system incorporates a collecting aperture (0.49 sq meters, 79-cm diameter) with an offset prime-focus configuration. It is fabricated using epoxy resin and carbon fibers, and the reflective surface consists of multiple layers of vapor-deposited aluminum and silicon dioxide.

The data system consists of two identical digital programmers, an analog multiplexer and two analog-to-digital converters (ADCs). The programmers provide. the redundant signals required to retrieve and format the radiometer and engineering data; provide signals to the ferrite radio frequency (RF) switches; initiate the integrate, hold and dump functions; and operate the ADC. They also interface to the satellite and receive clock, shift, and enable signals. On demand, they send instrument data to the satellite. The interface is also redundant (RIU A and B), and the instrument will operate with either programmer or satellite interface.

The analog multiplexer contains circuitry to provide very accurate temperature measurements of various RF loads and switches within the radiometers using platinum sensors. Also, the feed horn, sky calibration horns, and waveguide temperatures are monitored. Critical sections of the multiplexer are redundant to ensure reliability.

Thermistors are used as backup to the platinum sensors where critical temperatures are measured. The output of each radiometer channel is routed through the most significant multiplexer. Engineering data, such as mixer crystal currents and certain power supply voltages, are also multiplexed into the instrument t·data stream.

The power supply unit consists of independent power supply modules for each radiometer channel and data systems. Each supply is capable of being turned on and off separately and contains a number of isolated supplies, depending on its use. The over-voltage and current-limiting circuitry protects the switching regulators from potential harm. The switching regulators convert the dc input voltage to regulated ac voltage that is applied to a transformer with multiple outputs in one case and a single output in the other. The outputs are connected to dc series regulators and then to the radiometers and data system,

In summary, the TMR is operating extremely well and is providing a path delay correction less than 1.2 cm, No commands have been sent to the TMR since it was initially turned ON.

v. Global Positioning System Demonstration Receiver

The TOPEX/Poseidon mission includes an experimental Global Positioning System (GPS) precision orbit determination (POD) system that has now demonstrated a sub-3 cm accuracy in determining the orbit altitude. The GPS POD system is a global, differential, GPS system which features a GPS Demonstration Receiver (GPSDR) flight system and a global GPS tracking network with 14 stations. The system has demonstrated 1) the potential to supply sub-decimeter tracking data products quickly and inexpensively, and 2) the ability to provide 1.0 microsecond calibration of the satellite clock. Figure 17.0 depicts the system elements of the global GPS POD system.

The GPSDR is carried as a flight experiment on TOPEX/Poseidon to demonstrate the use of GPS for Precision Orbit Determination (POD) of satellites orbiting the Earth at low altitudes (200-6000 km). Developed by Motorola to JPL specification, the GPSDR is the first dual-frequency GPS receiver to be used for orbit determination with sub-decimeter accuracy. It is capable of tracking six GPS satellites simultaneously on both frequency bands (1.5 GHz and 1.2 GHz). Each band provides both pseudorange (P1 and P2) and carrier phase (L1 and L2) observable. Figure 18.0 show a schematic of the flight demonstration receiver architecture.

The on-board navigation solution makes it possible for the receiver to operate automatically. The solution provides doppler predicts for GPS satellite acquisition and the time-tag correction for the raw radio metric observable data. This time-tag meets 0.S μseconds accuracy virtually all of the time, versus 10 μseconds required for satellite clock calibration and 1μsec for time-tagging data). Ground processing also uses the on-board position solution to provide a-priori TOPEX/Poseidon positions to initialize the

precision orbit solution. During times when valid data are received from 4 or more satellites, the real-time position solution agrees with the post-fit precise orbit to about 100 m rms. Future missions are likely to rely on the on-board position for navigation.

To achieve sub-decimeter accuracy, the most important requirement is for the receiver to measure and put into telemetry carrier phase with 1 cm or better accuracy on both L1 and L2. Measurements are required on multiple GPS satellites simultaneously. Pseudorange measurements with decimeter accuracy are highly desirable. Accurate pseudorange allows automated data processing techniques to be used, which is highly desirable to handle the large volumes of data involved. The availability of high-quality pseudorange also enables accurate real-time navigation, and provides another data type for validation and enhancement of the carrier-phase-based solutions for the satellite orbit. The required and measured flight receiver precision and accuracies are given in Table 5.0.

Table S.0. Flight Receiver Errors

	Specified, cm	Measured, cm
Carrier Phase		
Systematic (LI & L2)	0.5	**<0.5**
Random (1 sec*)(L1& L2)	1.0	**0.2**
Pseudorange		
Systematic	**10.0**	**10.0**
Random (10 sec*)(P1& P2)	**19.0**	**16.0**
*** Noise integration time**		

The flight antenna is an important element of the system, To provide good geome ric strength to the orbit determination solution, GPS satellites must be tracked to low elevation angles. The specification is for a gain of at least -2 dBiC (dB relative to isotropic for circular polarization) at the L1 frequency, and at least -7 dBiC at the .2 frequency for elevation angles above 5°. A drooping crossed-dipole was used and mounted on a 30 cm diameter choke-ring backplane to electrically decouple the antenna from structures below the antenna. The location of the phase center of the antennas is calibrated with an accuracy of 0.5 cm, Remarkably, the variation between 5° elevation and 90° is 3,3 cm at L1 and 1,8 cm at 1..2. The L] phase calibration has a worst-case systematic error of .40 cm and a random error of 0.29 cm, For 1,2, systematic and random errors were 0.S6 cm and 0.23 cm.

In order to reduce multipath, and blockage from the 1.5-meter high gain antenna, the GPS antenna was mounted on a boom 4.3 m above the spacecraft body, Reflected GPS signals are received at the backside of the GPSDR antenna, however, gain is minimal due to the antenna sitting high on the boom. Figure 19.0 shows P1 multipath during a

track in which the GPS signal is reflected from a satellite surface. that results in meter-level multipath. Notice the characteristic temporal coherence between amplitude and delay variations during the period of strong multipath. The multipath during typical tracks is 10 cm rms with 100 second smoothing. Because of the relationship to measurable pseudorange multipath we know that the multipath on carrier phase must be less than 3 mm.

The flight receiver requires an initial upload from the ground to load ephemerides and to set the receiver clock. Once initialized, it is designed to operate autonomously, using TOPEX/Poseidon position solutions and GPS ephemerides to generate estimates of doppler to aid GPS acquisition, The receiver calculates GPS view periods, and a set of 6 is chosen based on length of track, mutual visibility with ground stations, and geometric strength. If 6 GPS satellites are not available, the receiver assigns multiple channels to track the same satellite. On a typical day, each channel was locked to a satellite for 98% of the time, with about 2% of time spent in the acquisition mode.

To achieve 3 cm accuracy for the altitude of TOPEX/Poseidon, a 14 ground station GPS global tracking network has been used. This network consists of six Rogue SNR-8 receivers operated under the auspices of the NASA's offices of Space Communications and eight more that are part of the new IAG-sponsored International GPS Service due to begin in 1994. The Rogue SNR-8 provides dual-band, high-precision pseudorange and carrier-phase observable. The receivers are operated in collaboration by CEE (Chile), CNES (France), and ISAS (Japan), and NASA/JPL (USA), NASA operated three receivers at the Deep Space Network (DSN) sites located at Goldstone, California; Madrid, Spain; and Tidbinbilla, Australia. CEE, CNES, and ISAS each supported a Rogue station at Santiago, Chile; Hartebeesthoek, South Africa; and Usuda, Japan. The operational support of the ground network was agreed upon in Letters of Agreement (LOA) between 'NASA and CEE, CNES, and ISAS. According to the agreement, NASA collected the data daily from all 6 sites and transferred it to the GPS Data Handling Facility (GDHF) at JPL for processing, distribution, and analysis, while the DSN, CEE, CNES, and ISAS maintained and operated their respective field sites,

The TOPEX/Poseidon mission requirements from the GPS 6-station network is outlined in Table 6.0. The mission required GPS data from 9 full segments of 10 days each from both the ground network and from the flight receiver over a period of 6 months (hence about 50% of the data). The GPS receivers were required to provide GPS observable every 30 seconds in 24-hour files (generally uploaded once per day). The data was to be provided to the GDHF within 7 days of receiver acquisition and consequently the mean time to repair (MTTR) was limited to 7 days. The operations of the Network achieved all of the stated mission requirements. From the official mission start, 02 November, 1992 to the end of the experimental phase in May, 1993, the 6-station network collected about 9570 of the expected data quantity. The expected quantity was derived from a month-long average of data collected from each station. The data was on average obtained within 36 hours from generation in the GPS receivers, which is well within the

7-day goal. GPS observable residuals from post-filter analysis of the GPS data is an indication of GPS observable data noise. These residuals were 3-4 mm for carrier phase observable and about 20 cm for pseudorange observable. These residuals were routinely monitored at the GDHF, in addition to data file sizes, and other data validation indicators,

Table 6.0. Network Requirements for TOPEX/Poseidon (6 stations)

	T/P (6 sites)
Data Latency	7 days
Mean Time To Repair (MTTR)	7 days
sample rate	30 seconds
data products	14 days
Internet Communications	NO

While the six-station network has been the primary focus of the experiment in evaluating the operational potential of the GPS-based POD system, the incremental cost of getting data from the 14-station network to support the 3 cm or better orbit accuracy has proven to be very low.

VI. Laser Retroreflector Array

The Laser Retroreflector Array (LRA) interfaces with the ground-based Satellite Laser Ranging (SLR) tracking stations for height verification and POD. The LRA design consists of a conical configuration, mounted around the altimeter antenna, as was used on SEASAT, The retroreflector cube corners are mounted in twelve trays, in two rows, which form the conic section. A total of 216 cube corners were used in the LRA design (SEASAT used 96 cubes). The LRA uses cube corners of the SEASAT design, They have a hexagonal aperture of 3.8 cm across, and are oriented on the satellite such that all 216 cubes are at 40° (±1 deg) from the satellite nadir. This offset angle arrangement provides adequate cross section for elevation angles of 20° or greater. Figure 20.0 provides a conceptual view of the assembled LRA torodial ring and appears very much as it would if one were looking up at the satellite. The LRA trays are virtually identical to each other in construction. Each element consists of a laser retroreflector segment that houses a mounting tray approximately 5 inches wide,

The overall performance requirement for the LRA is to be capable of supporting ranging data with an uncertainty of ±3 cm and absolute calibration over the verification site to ± 2 cm. The LRA is a bright retroreflector that provides strong signal return which is attenuated by the ground laser receivers, Typically the SLR network ranging systems perform better than these requirements,

VII. Frequency Reference Unit

The Frequency Reference Unit (FRU) provides the ultrastable time reference to the satellite and the NASA sensors. The two CNES instruments use an ultrastable oscillator (USO) built into the DORIS receiver. A functional diagram of the FRU and the 3 stable frequencies output to the users is shown in Figure 21.0. The redundant elements and cross-strapping are not shown for simplification purposes. The FRU consists of a 5 MHz oscillator, two frequency synthesizers operating at 19.0S6 MHz and 4.096 MHz, and the frequency distribution unit. The 5 MHz oscillator utilizes a BVA design, 3rd overtone, SC (stress compensated) cut quartz resonator maintained at a constant temperature to achieve the frequencies and frequency stability required by the satellite and sensors. A BVA design is unique because the electrodes which make connections to the piezoelectric quartz are not deposited on the critical frequency determining area of the quartz. The two frequency synthesizers are of a similar design in that a voltage controlled crystal oscillator (VCXO) is driven by the output of a phase comparator in a phase locked loop. The phase comparators use the 5 MHz and the respective VCXO output, each divided by a unique integer to a common submultiple frequency, to provide the control voltage. The VCXOs use an FC cut quartz resonator in a temperature controlled oven. On a long term basis, the VCXOs achieve the frequency stability of the 5 MHz BVA oscillator.

The frequency distribution unit provides buffering between the loads and the frequency sources and matches the load requirements for levels, waveforms and impedances. As can be seen in Figure 21.0 there are multiple users of the three FRU output frequencies. The NASA altimeter uses the 5 MHz output for its basic timing and height determination. Since the round trip light time for TOPEX/Poseidon is less than 10 milliseconds, the altimeter imposed a 10 millisecond short term stability requirement on the FRU. This was considered to be the driving requirement on frequency stability. The S-band transponder uses the 19,056 MHz to phase lock a voltage controlled oscillator to generate the basic timing reference for S-band frequency generation when operating in a non-coherent mode with a ground tracking station or with the Tracking and Data Relay Satellite System (TDRSS). The Doppler data recovered from the carrier frequency in this non-coherent mode, referred to as one-way Doppler, is the data type used for orbit determination to support the mission operations activities. The orbit solution activities using the one-way Doppler results in a measurement of the S-band carrier frequency. The carrier frequency is algorithmically derived from the 5 MHz oscillator through the design equations of the 19.0S6 MHz synthesizer and the transponder. It is possible, therefore, to accurately calculate the actual operating frequency at the 5 MHz oscillator on a daily basis.

The GPSDR utilizes the 4.096 MHz frequency for its basic timing and internal clock, The GPSDR provides a determined orbit solution every 10 seconds when tracking four or more (capability of up to six concurrent) GPS Navstar satellites, A part of the orbit solution is the offset of the internal GPSDR clock, derived from the FRU 4.096 MHz,

from the GPS system time. This is a direct measurement of the offset of the 4.096 MHz frequency which, since the 5 MHz and 4.096 MHz are phase locked, provides a second measurement of the actual operating frequency of the 5 MHz oscillators.

The Instrument Module Interface Unit (IMIU) also uses the 4.096 MHz for the basic timing of its internal digital circuitry. Included in this digital circuitry is the satellite clock which is used to time tag the. engineering and science data. The clock consists of a 48-bit binary counter which accumulates counts at a 1.024 MHz rate counted down from the 4.096 MHz frequency. This clock is read out in telemetry at a regular basis and is correlated to UTC (coordinated universal time) by ground processing.

The Central Unit (CU) is the third satellite user of the 4.096 MHz. The CU also provides a 1,024 MHz clock to the TOPEX Microwave Radiometer (TMR) through the satellite multiplexed data bus (MDB). The CU has the capability of operating either on its own internal oscillator or an external oscillator (FRU). The CU is responsible for decoding and distributing commands to the various satellite components and sensors via the MDB and also acquiring telemetry data via the MDB. The CU formats the telemetry data for transmission to the operations center. The CU normally is operated on the external FRU 4.096 MHz in which case the entire satellite, except for the two CNES sensors, is operating synchronously from the FRU outputs.

The performance of the 5 MHz oscillator in the FRU has been excellent for both the operating frequency and frequency stability. A plot of the 5 MHz frequency offset in milliHertz since launch is shown in Figure 22.0. The offset is defined as negative because the actual frequency is less than 5 MHz by the amount shown for any given day. The plotted data are obtained from the one-way Doppler data as part of the orbit determination activity and represent daily average offsets. Several things should be noted on Figure 22.0. First, the aging drift rate became less than the specification for the 24 hour drift rate of less than 7.7 x 10-11, about a week after launch. The drift rate decreased as the oscillator reached temperature equilibrium and began the anticipated aging cycle. The aging induced drift rate went from positive, through zero to negative in July 1993. The aging drift rate shows an influence associated with the flask temperature. This is a temperature measurement external to the oven flask used with the 5 MHz oscillator. This temperature shows periodic variations associated with the orbit precession and the satellite attitude control modes. The correlation of offset changes with temperature variations is clear and consistent. However, the amount of change, while somewhat greater than anticipated from prelaunch testing, is too small to affect performance. there is some concern that the total integrated radiation dose at the TOPEX altitude (1336 km) may be a factor in the resonator aging process. The satellite has no means to directly measure that parameter. In summary, the performance of the FRU since launch continues to be excellent and is performing better than the specification.

VIII. Performance Summary

Outstanding satellite and sensors performance. is indicated across all subsystems. This is being evidenced in overall mission performance in several basic ways:

a. Satellite is properly maintaining the altimeter pointing.
b. Approximately 99% of the science data are being returned and placed on the GDR in a timely manner.
c. All satellite subsystems except for the ASTRA 1-B star tracker are performing better than specifications.
d. All sensors are performing better than specifications.
e. Four Orbit Maintenance Maneuvers have been performed with increasing accuracy and at 10-day cycle boundaries farther apart than predicted.

Further illustration of the successful operation and performance of the satellite and sensors is given in Table 7.0, where a summary of requirements specifications and actual on-orbit performance are presented for comparison purposes.

In closing, some of the highlights of the TOPEX/Poseidon mission thus far are:

a. Successful launch August 10, 1992.
b. Completed six orbit maneuvers in seven weeks to reach the observational orbit in 43 days, September 1992.
c. Satellite attitude control adjustments were determined and implemented to achieve precise pointing for improved observations beginning December 1992.
d. A successful Verification Workshop was conducted February 1993, culminating in the final ground algorithm corrections for science processing.
e. Good mission performance has been achieved by careful monitoring of the ground track and performing orbit maintenance maneuvers,
f. The satellite batteries have performed well as a result of following operations procedures recommended by the Battery Team.
g. IGDR/GDRs have been prepared and delivered consistently ahead of schedule, the mission is benefiting by getting timely feedback from Principal Investigators.
h. NASA Radar Altimeter and TOPEX Microwave Radiometer performance is better than specifications.
i. As reported by CNES, both DORIS and SSALT are performing better than specifications.
j. Single Event Upsets induced by radiation at the satellite altitude have not caused serious and sustained data outages.
k. The GPS Experiment was completed successfully in May 1993. GPS orbits for nine 10-day cycles were released to the science community, these orbits were accurate to about 3 cm in the radial component. Additionally, the flight receiver has been reprogrammed to successfully track in the coarse acquisition mode which means the receiver can use GPS constellation data all the time.
l. The Flight Team has done a superb job of keeping the satellite within the ± 1 km ground track which is required to continuously make the topographic

measurements at nearly the same spot over a long duration. Refer to Figure 23.0 for a history of the ground track thus far in the mission.

Lastly, the mission objective is to measure the ocean topography with an uncertainty of 14 cm. The measurements placed on the GDRs have now been verified to generally be about 6 cm or better, as shown in Table 8.0. This is indeed a tribute to the performance of all subsystem elements and the combined efforts of the joint U.S. and French TOPEX/Poseidon Project personnel.

Ix. Acknowledgments

Particular gratitude and appreciation are extended to the development, integration, test, launch, and all operations support groups which have made this mission possible.

For the NASA Radar Altimeter, the authors want to acknowledge Laurence C. Rossi, David W. Hancock III, George Hayne, and Ronald Forsythe of the Goddard Space Flight Center; and Paul Marth of the Johns Hopkins University/Applied Physics Laboratory for their contributions.

For the TMR, we appreciate the contributions of Floyd G. Olson and Edward J. Johnston of the Jet Propulsion Laboratory.

For the GPS POD system, the authors want to acknowledge, Tim Munson, Larry Young, Keith English, Ulf J. Lindqwister, and Charlie Dunn, all of the Jet Propulsion Laboratory, for their work in calibrating the flight equipment.

The work described in this paper was conducted under management by the Jet Propulsion Laboratory, California Institute of Technology, under contract with the National Aeronautics and Space Administration.

X. References

L. Carson, L. Hailey, G. Geier, R. Davis, G. Huth, T. Munson, "Design and Predicted Performance of the GPS Demonstration Receiver for the Nasa TOPEX Satellite," *Position Location and Navigation Symposium*, pp. 442-454, 1988 PLANS.

G. C. Cleven, *Satellite Time Correlation and FR U Performance Assessment Functional Requirements,* JPL Internal Document D-8485, Rev. A, Jet Propulsion Laboratory, Pasadena, CA, September 1993.

L. -1.. Fu, E. J. Christensen, M. Lefebvre, and Y. Menard, *TOPEX/Poseidon Mission Overview,* preprint for JGR Spring 1994.

xl. Tables

Table 1.0 NASA Radar Altimeter Characteristics

Item	Parameter	Description
Transmitted Waveform	Chirp modulation	Linear FM sweep
	Center frequency	13.6 GHz (main), 5.30 GHz 102.4
	Pulse width (PW)	μs
	Bandwidth (BW)	320 MHz
	Pulse period	204.8 μs
	Burst period (1334 km)	8893 p s
	Pulse repetition freq.	4200 (Ku), 1220 (C)
Antenna	Type	1.5-m parabola
	Gain	43.9 dB (Ku), 35,7 dB (C)
	Beamwidth	1.1 deg (Ku), 2.7 deg (C)
	Footprint	26 km (Ku), 61 km (C)
Transmitter	Peak power	20 W (Ku), 20 W (C)
Signal Processor	Waveform samples	128 per channel
	Range resolution	0.5 m
	'l'racker type	Alpha-Beta
Operation Modes	Idle	CNESSSALT ON
	Standby	Not transmitting
	Track	4 track modes
	calibrate	4 calibrate modes
	Test	4 test modes
Inputs	Power bus	23-35 V dc
	Timing signal	5MHz (0.8 V p-p)
	Commands	Relay (20, 1/s), Data (16-b, 1kb/s)
outputs	Telemetry	1228 byte frame
	Rate	About 9,8 kb/s

D. W. Hancock, G. S. Hayne, J. B. Bull, R. L. Brooks, C. L. Purdy, *TOPEX Mission Radar Altimeter Engineering Assessment Report*, Sep. 93.

J. R. Norton, "BVA-Type Quartz Oscillator for Spacecraft," Enclosure 1 to TSSD-15904, Johns Hopkins University/Applied Physics Laboratory.

M. J. Reinhart, *A Space-Qualified Frequency Synthesizer, 52 R-91-092,* Johns Hopkins University/Applied Physics Laboratory.

TOPEX/Poseidon Satellite/Sensors Performance Characteristics Workshop #2, JPL Internal Document TPO 93-254, Jet Propulsion Laboratory, Pasadena, CA, September 15, 1993.

TOPEX/Poseidon Verification Workshop, Summary Report, JPL Internal Document D-10815, Jet Propulsion Laboratory, Pasadena, CA, May 24, 1993.

A. R. Zieger, D. W. Hancock, G. S. Hayne, and C. L. Purdy, "NASA Radar Altimeter for the TOPEX/Poseidon Project," *Proceedings of the IEEE,* Vol. 79, No. 6, June 1991.

Table 2.0 NASA Radar Altimeter Specifications and On-orbit Performance
for 2, 4, and 8 **Meter Significant Waveheights**

	Significant Waveheight					
	2M		4M		8M	
	Spec	On-orbit	Spec	On-orbit	Spec	On-orbit
Combined	4.1	1.4 -2.9	4.6	2.2 -3.3	5.5	3.7 -4.5
Ku	3.5	1,2 -2.4	3.6	1.8- 2.'?	4.5	3.1 -3.8
C	5.4	1.8 -3.7	6.1	2.9 -4.4	7.4	5.1 -6.3
One-Second Range Measurement Noise Performance (in cm)						

Table 3.0 Comparison of TMR Parameters and Functional Requirements

PARAMETERS	CHANNEL 1	CHANNEL 2	CHANNEL 3	CHANNEL 4
Channel Frequency (GHz)				
Specification	18,0 ±20	21.0 ±20	21,0 ±20	37.0 ±20
Measured	18,004	20.999	20.994	36.997
Temperature Resolution A']'				
Specification	≤0.4	≤0.4	≤0.4	≤0.4
Measured	0.26	0.27	0.27	0.27
Near Sidelobe Beam Fraction %				
Specification	≤3.0	≤3.0	≤3.0	≤3.0
Measured	2.7	2.5	3.1	2.2
Far Sidelobe Beam Fraction %				
Specification	≤7.0	≤6.0	≤6.0	≤5.0
Measured	0.7	0.4	0.s	0.7
IF Bandwidth (MHz)				
Specification	100 ±10	100 ±10	100 ±10	100 ±10
Measured	10s	105	105	105
Dynamic Range (Kelvin) Min				
Specification	330	330	330	330
Measured	400	400	400	400
Absolute Accuracy (Kelvin)				
Specification	1.0	1,0	1.0	1.0
Measured	0.27	0.27	0.27	0.27

'I'able 7.0 Performance Versus Requirements

Key Requirement	Performance
Mission requirement to return 81%/ of data to GDR	Meeting: Greater than 99% science return to G DR
Point the altimeter antenna 0.08° or better, 1 sigma	Meeting: Since Dec. 24, 1992 typically point 0.05° or better
Maintain observational orbit ground track to ± 1 km	Meeting: 989% of all nodal crossings have been less than ± 1 k m
Correlate time to 100 micro seconds	Meeting: Since Sept. 23, 1992 the satellite time to UTC has been correlated to less than 10 micro seconds
Provide lifetime of 3 years or more	Actions taken to extend lifetime — Battery management, keep charging current low by offsetting array to sun — Reduced High Gain Antenna position mot ion — Developed backup attitude control mode in event of star tracker failure

Table 8.0 Preliminary Assessment of Measurement Accuracies (one sigma values in cm)

	Performance	Requirement
Altimeter Range		
Altimeter noise[1]	1.7	2,0
EM Bias	2.0	2.0
Skewness[2]	1.2	1.0
Ionosphere[3]	0.5	2.2
Dry Troposphere	0.7	0.7
Wet Troposphere	1.2	1.2
Total Altimeter Range[4]	3.2	4.0
Radial Orbit Height[5]	**4.7**	**12.8**
Single Pass Sea Height	**5.7**	**13,4**

(1) Altimeter noise is based on 3-see average and significant wave height (SWH)=2 m.
(2) Not well determined for SSALT
(3) Use 2.(I cm for I> C) RIS-bawd correction
(4) Altimeter bias and bias drift not included
(5) Post verification workshop estimate based on the JGM-2 gravity model

XII. Figures

Figure 14.0 The TMR consists primarily of an antenna, RF section, and digital section. The TMR is tipped 42 degrees when mounted to the Instrument Module to align the beam vertically.

Figure 15.0 The TMR Functional Schematic Diagram illustrates the 4 channel design and connections with the multi-frequency feed horn and the sky calibration horns.

Figure 16.0 Typical Dicke switch radiometer channel design used in the TMR.

Figure 17.0 The GPS POD system is a global network of GPS satellites, ground based GPS receivers, the satellite flight receiver, and ground operations.

Figure 18.0 The schematic shows the flight system GPS Demonstration Receiver fundamental architecture.

Figure 19.0 PI multipath and SNR taken from flight data are shown vs time. The multipath observable is the linear combination of pseudorange and carrier phase observable which removes the effects of geometry, clocks, and ionosphere, leaving primarily multipath, along with system noise and systematic errors. Ten second normal points are plotted.

Figure 20.0 LRA as it would appear looking up at the satellite.

Figure 21.0 The FRU functional diagram and outputs to the NASA altimeter (5 MHz), satellite primary references (4.096 MHz) and satellite transmitter (19.056 MHz).

Figure 22.0 The 5.0 MHz Offset in MilliHertz Shown Since Launch

Figure 23.0 The satellite ground track is controlled by performing Orbit Maintenance Maneuvers (OMM) to stay within the ± 1 km measurement zone.

XII. Figures

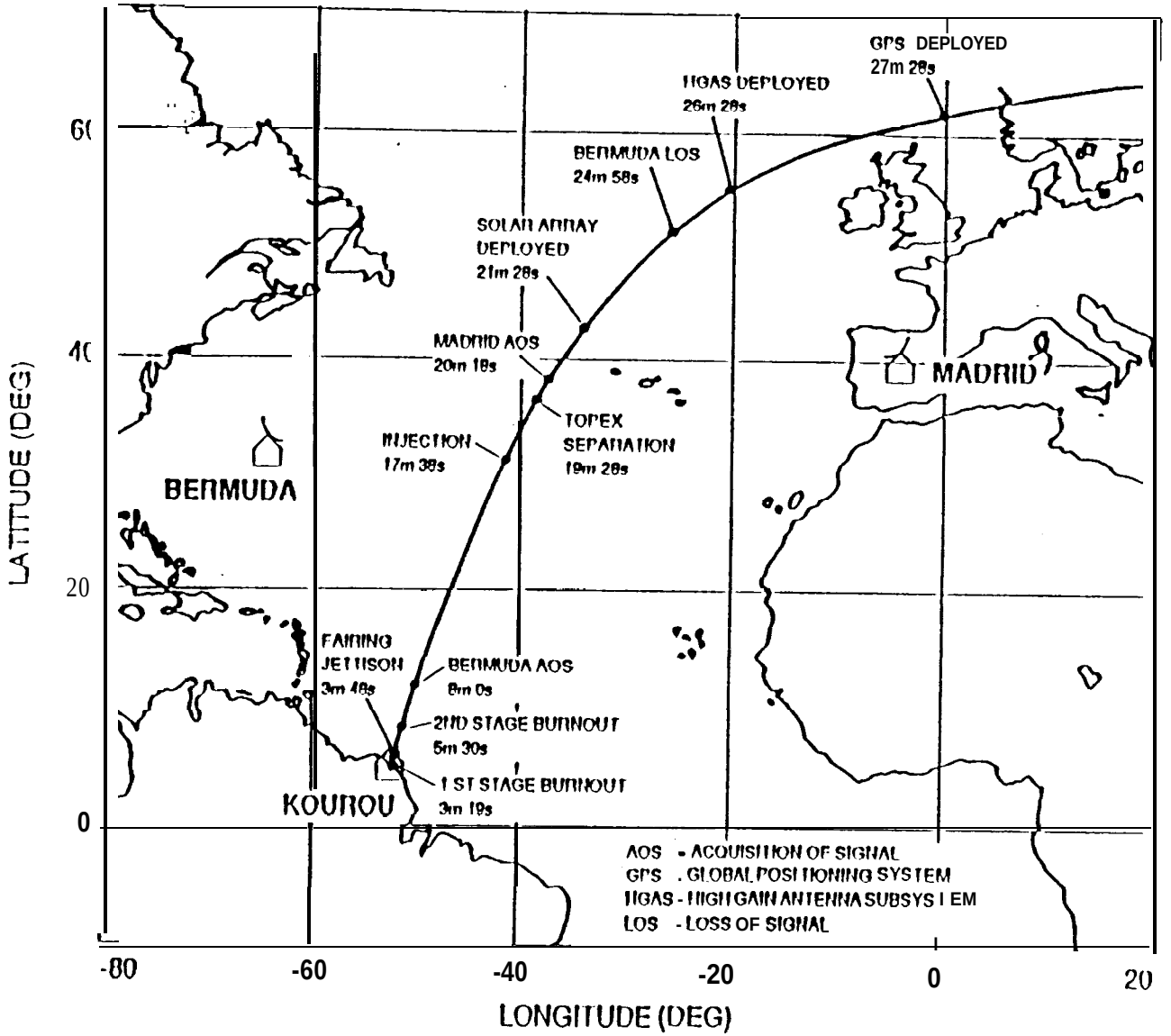

Figure 1.0 **The satellite rose from Kourou during a spectacular night launch and was carried northeast by the Ariane 42P to an altitude of about S30 miles.**

TOPEX/POSEIDON PROJECT DEVELOPMENT AND OPERATIONS SCHEDULE

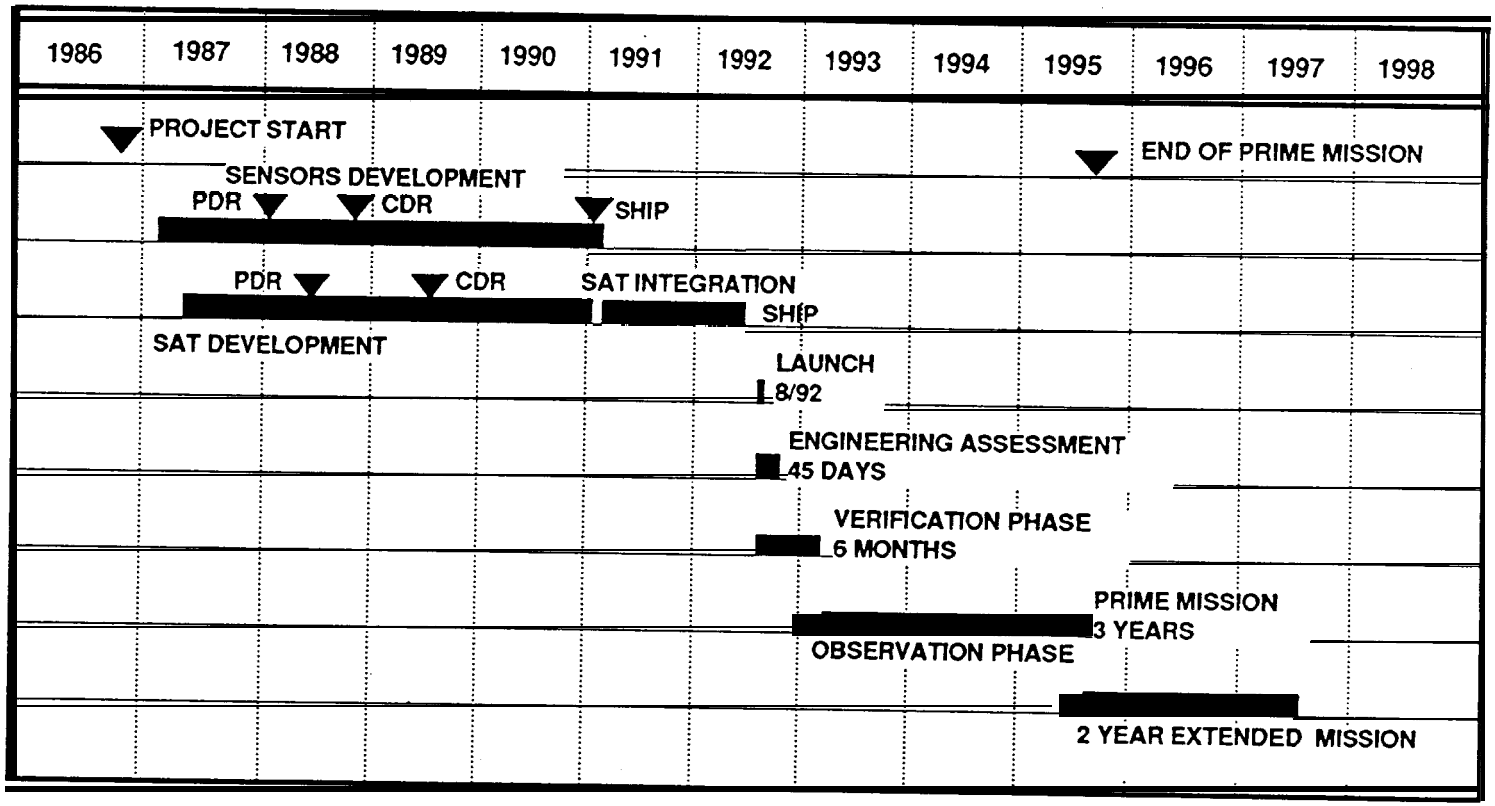

Figure 2.0. Satellite and Sensors Development, Integration, Test and Mission Operations

INSTRUMENT MODULE AND MULTI-MISSION MODULAR SPACECRAFT

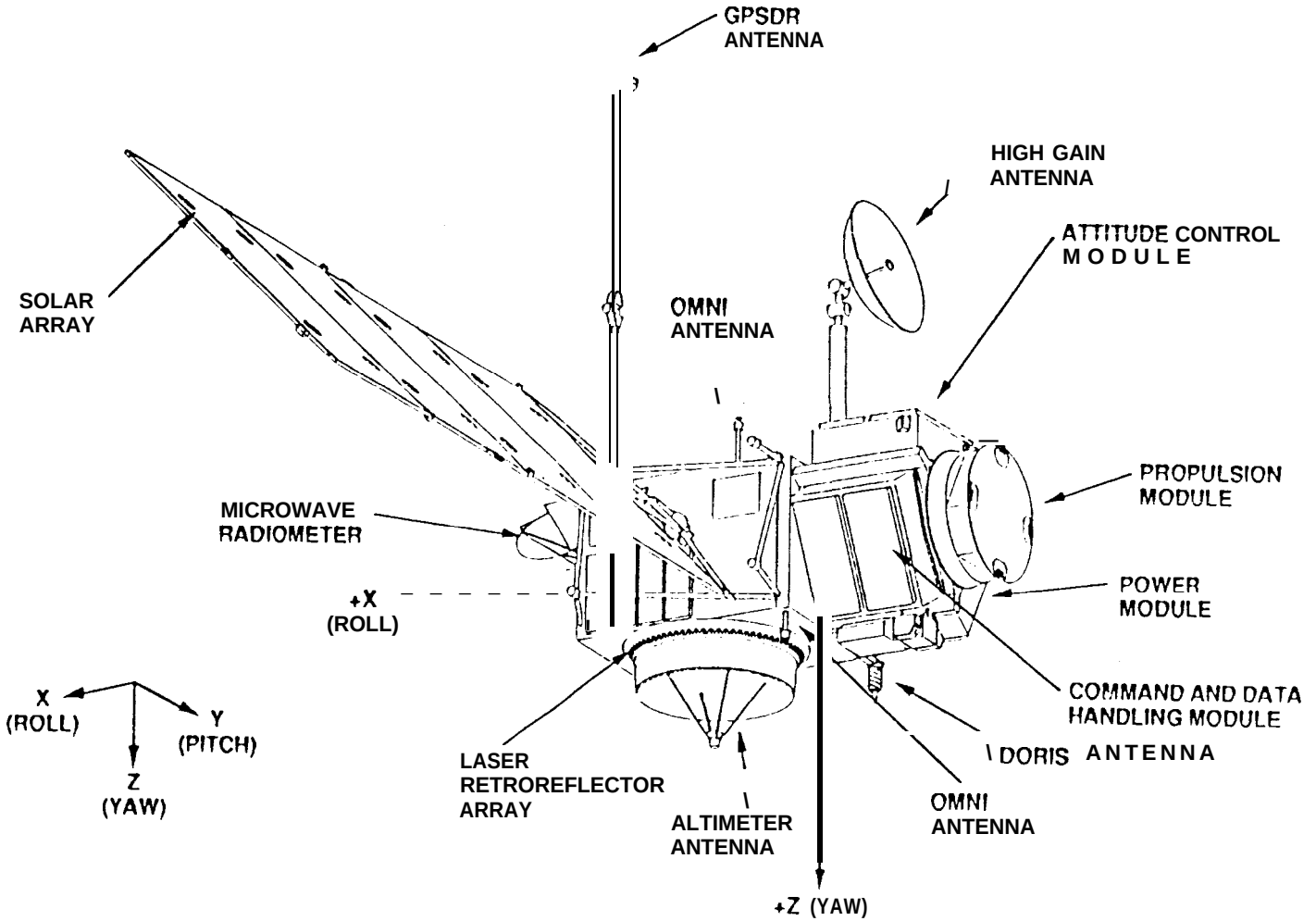

Figure 3.0 Satellite Configuration and Payload Sensors

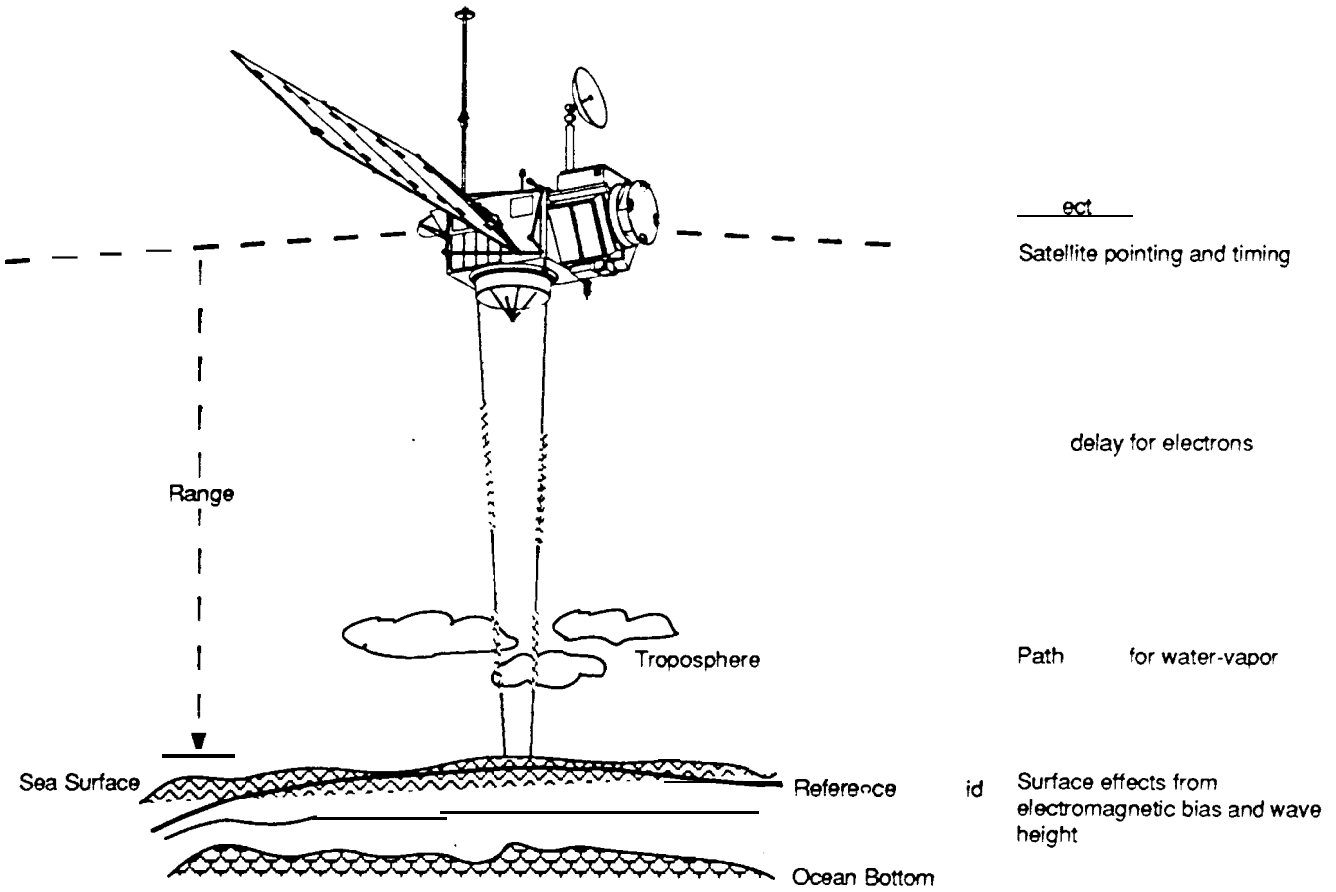

Figure 4.0 The altimeter range measurement and corrections are illustrated schematically to show the geometry of the measurement.

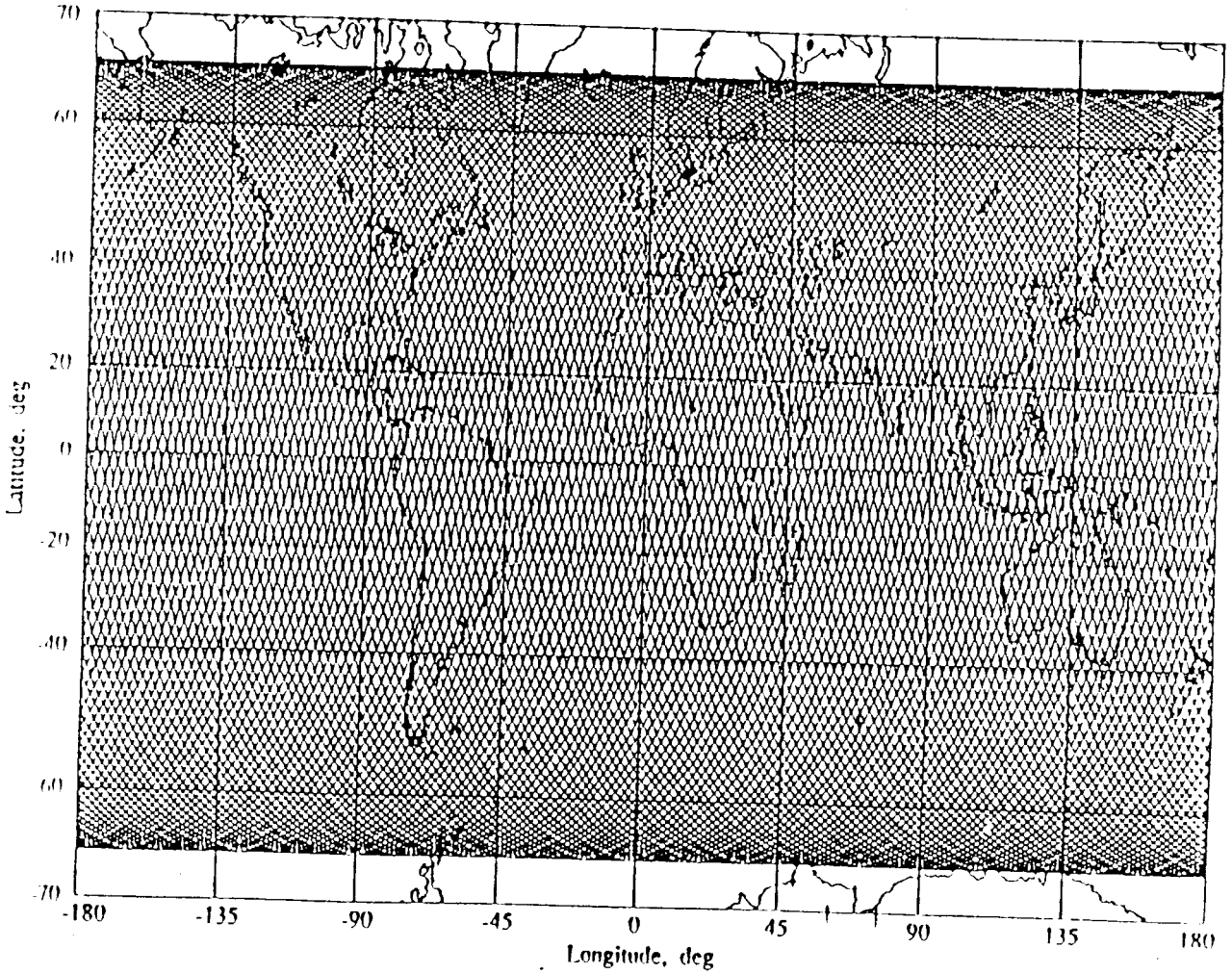

Figure 5.° Ground Track of °-day Repeat Observationa Orbit Cycle (127 revolutions)

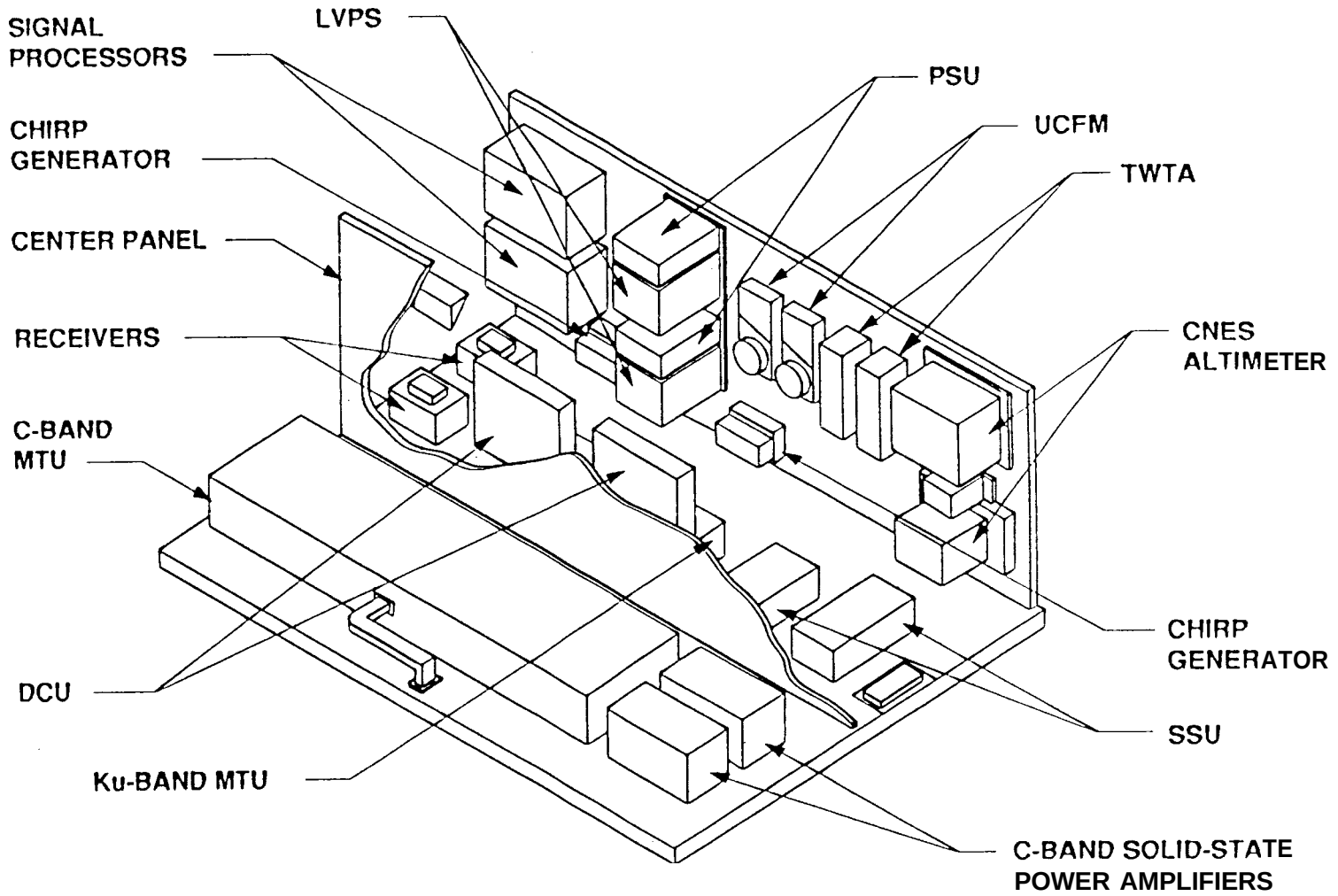

Figure 6.0 The altimeter subsystem components are mounted in the F-Section of the Instrument Module Structure.

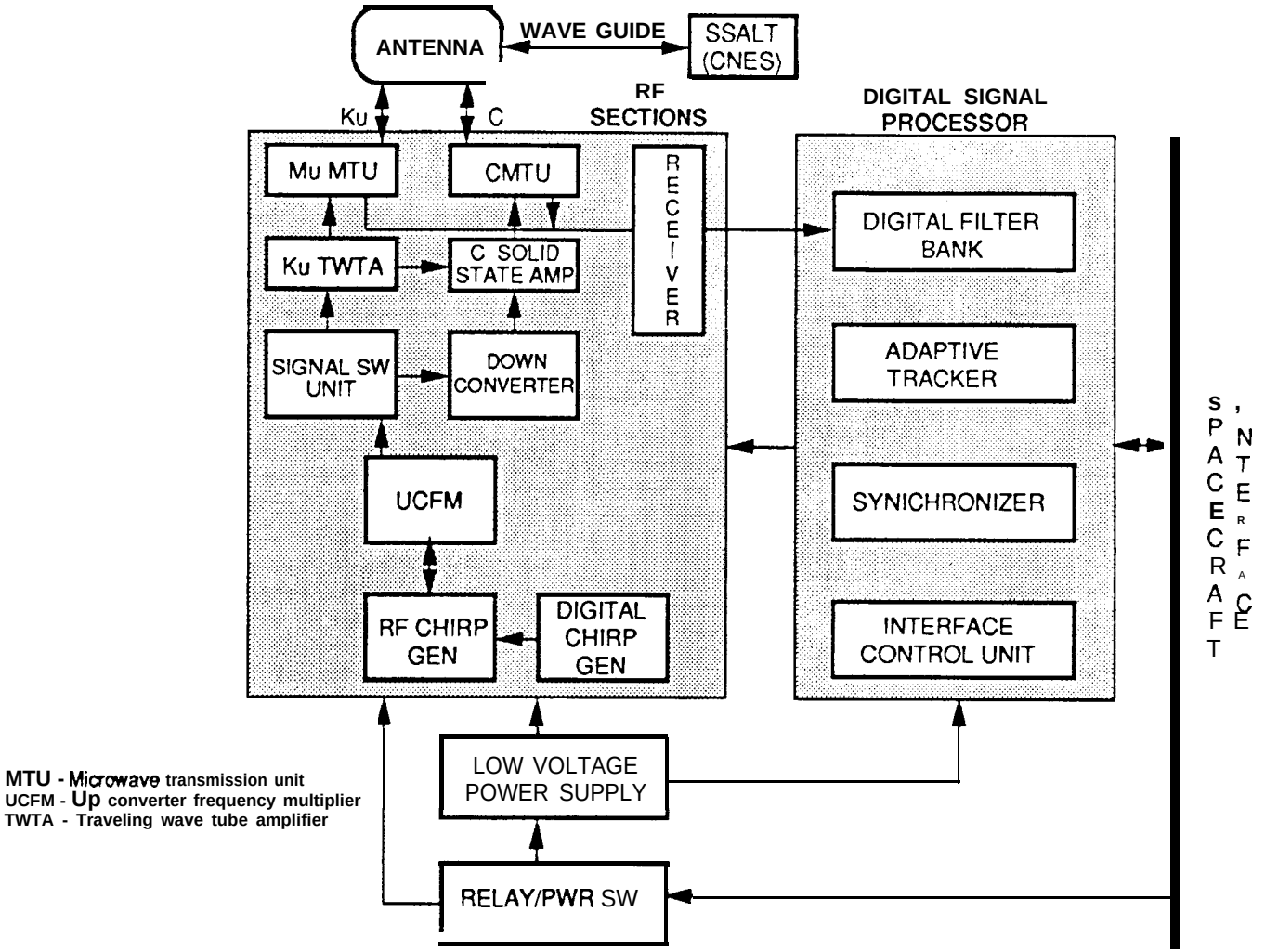

Figure 7.0 The functional block diagram of the NRA which has Side A and Side B redundancy.

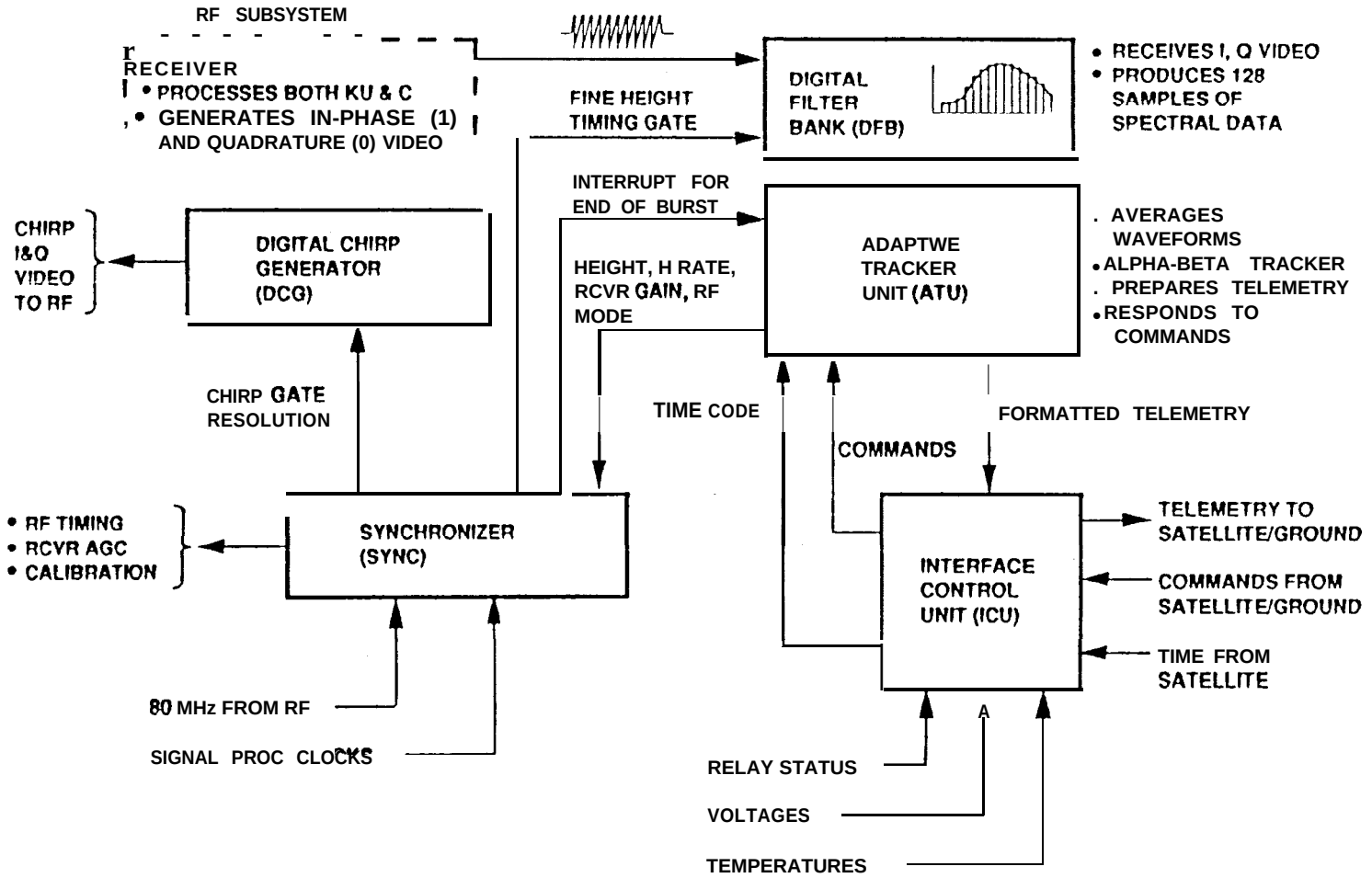

Figure 8.0 **The all digital signal processor converts I and Q video signals from the receiver into digitized waveforms, computes the height measurement, generates the telemetry output, and processes altimeter commands.**

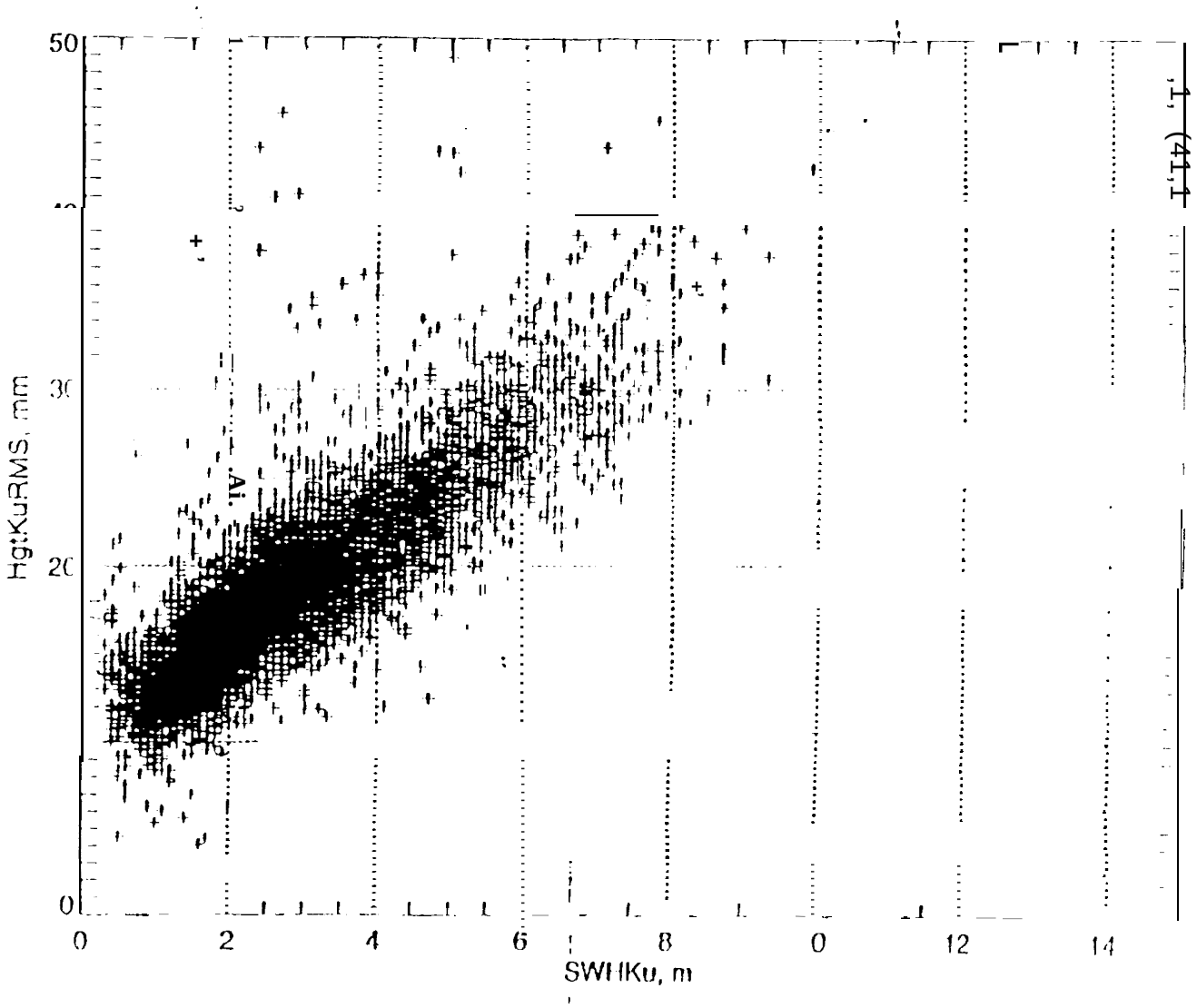

Figure 9.0 Height Noise Versus Significant Wave Height

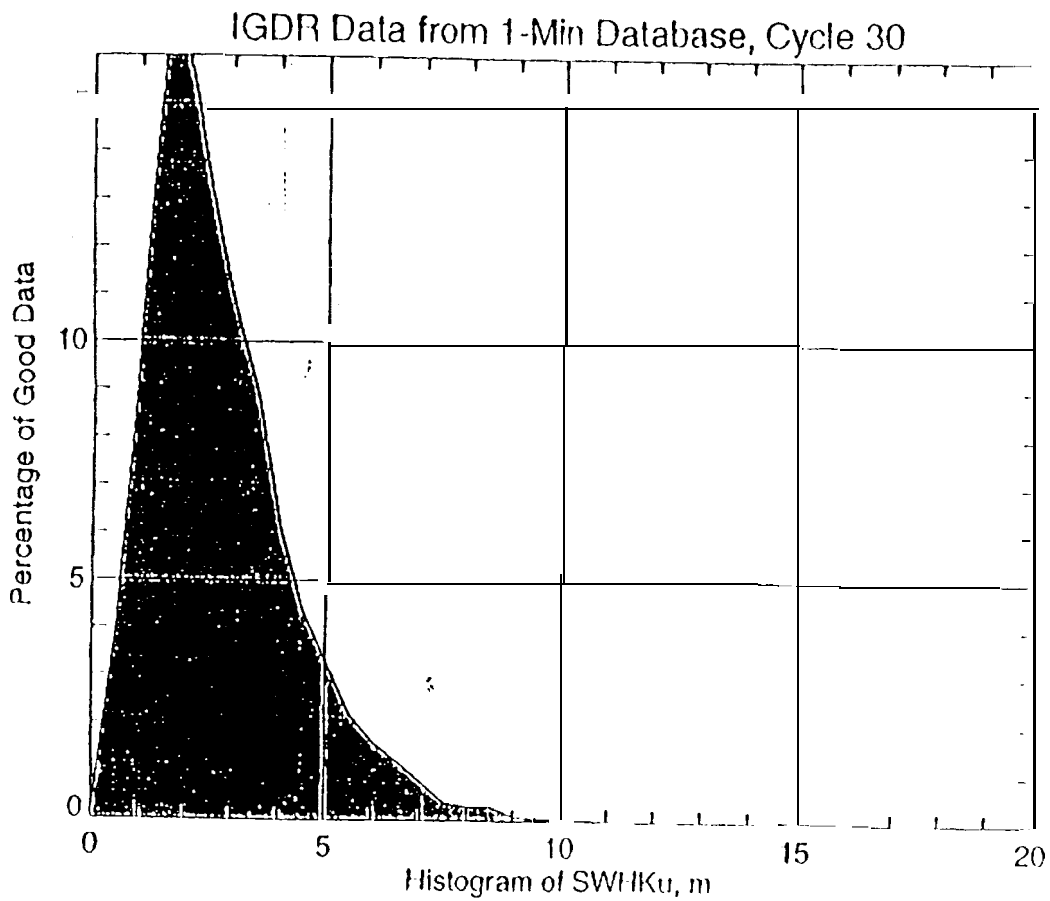

Figure 10.0 Histogram of Significant Waveheight Measurements for Ku-band

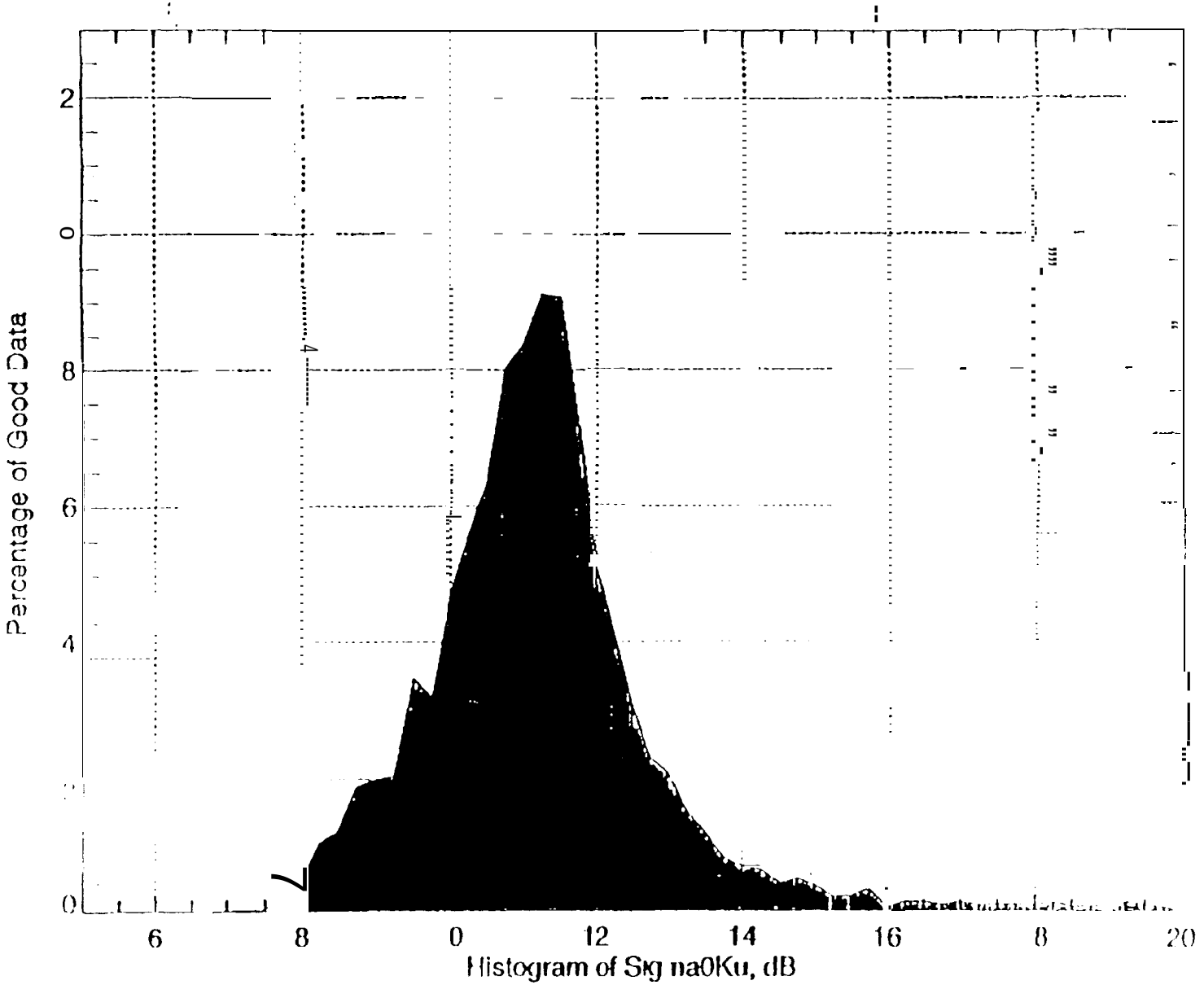

Figure 11.0 The percentage of good data for sigma-naught ku-band a full 10-day cycle of data.

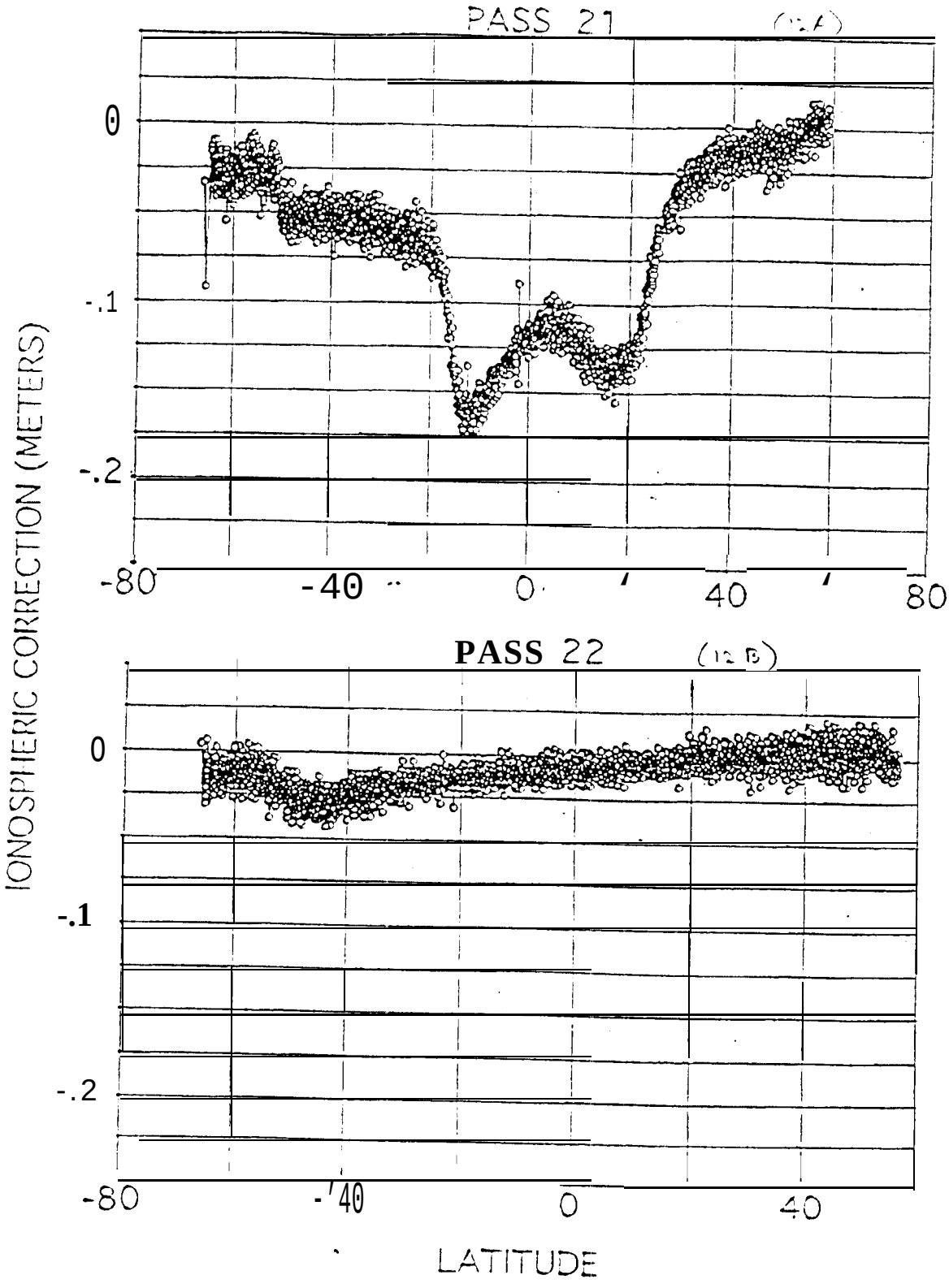

Figure 12.0 **A and B shows the ionosphere correction for 2 passes or 1 complete orbit. Pass 21 shows the much larger correction required for the daytime portion of the orbit.**

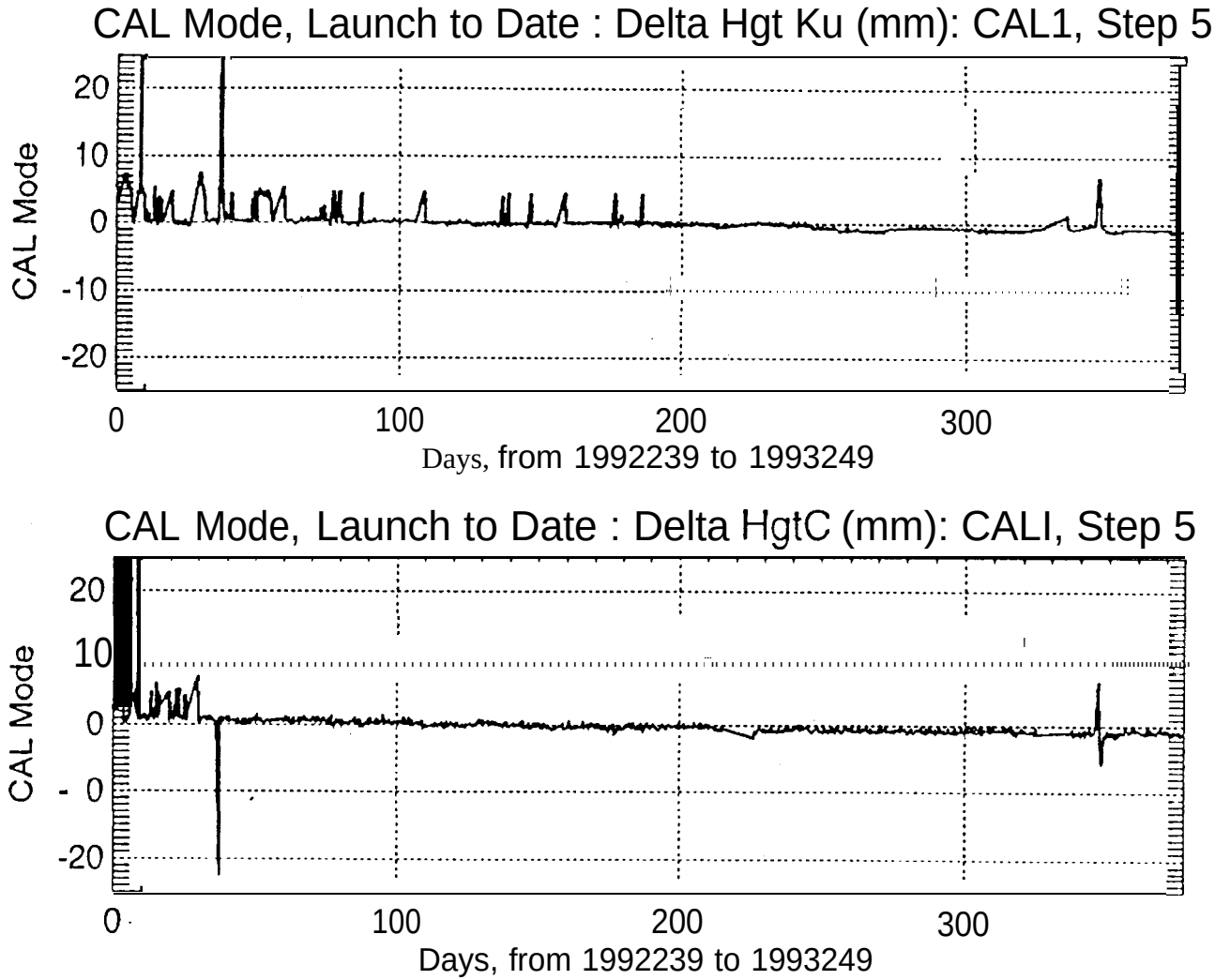

Figure 13.0 The calibration mode for **Ku and C-band indicates** there **has been no discernible drift in the height bias.**

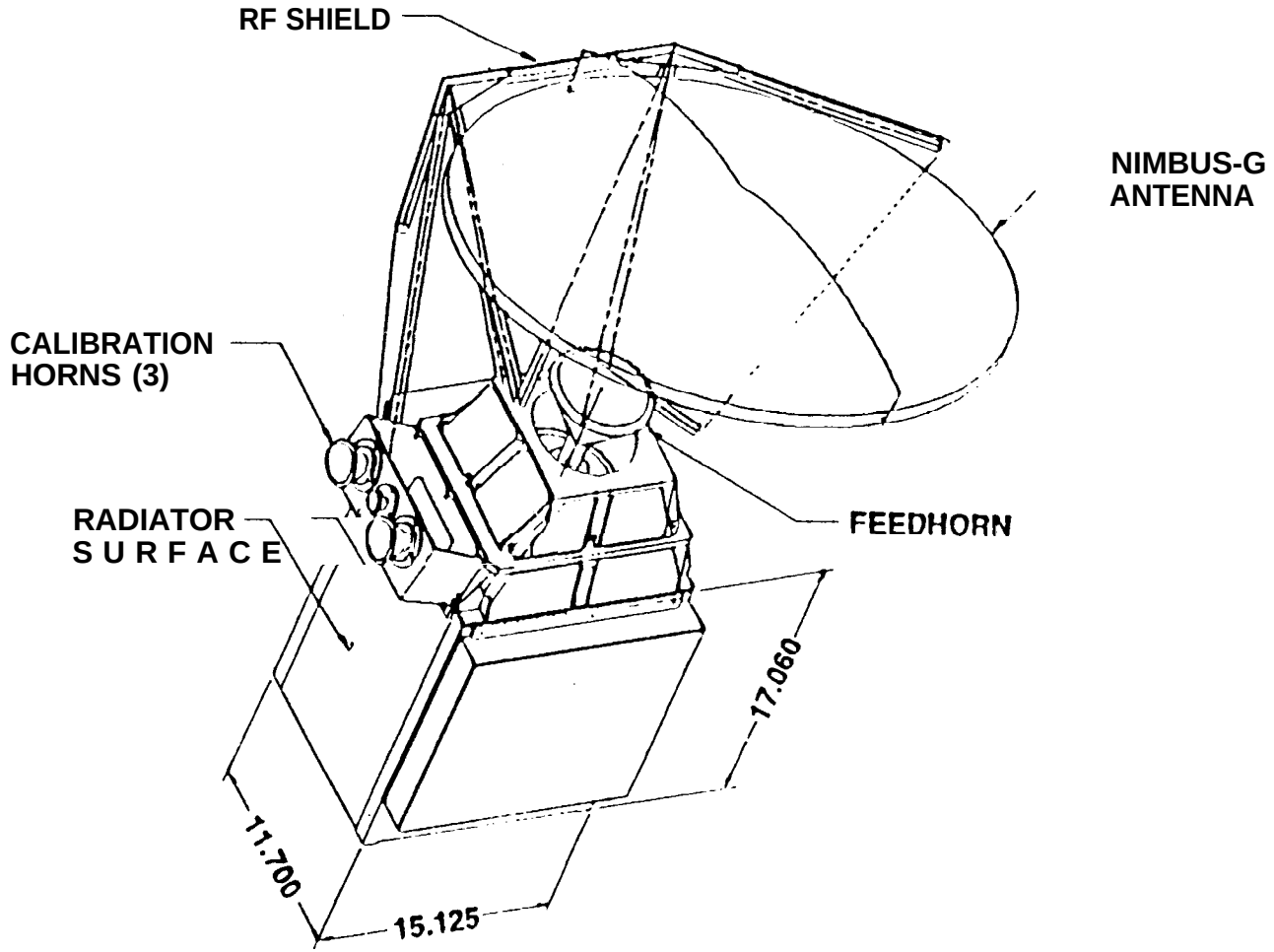

Figure 14.0 The TMR consists **primarily of an antenna, RF section, and digital section. The TMR is tipped 42 degrees when mounted to the Instrument Module to align the beam vertically.**

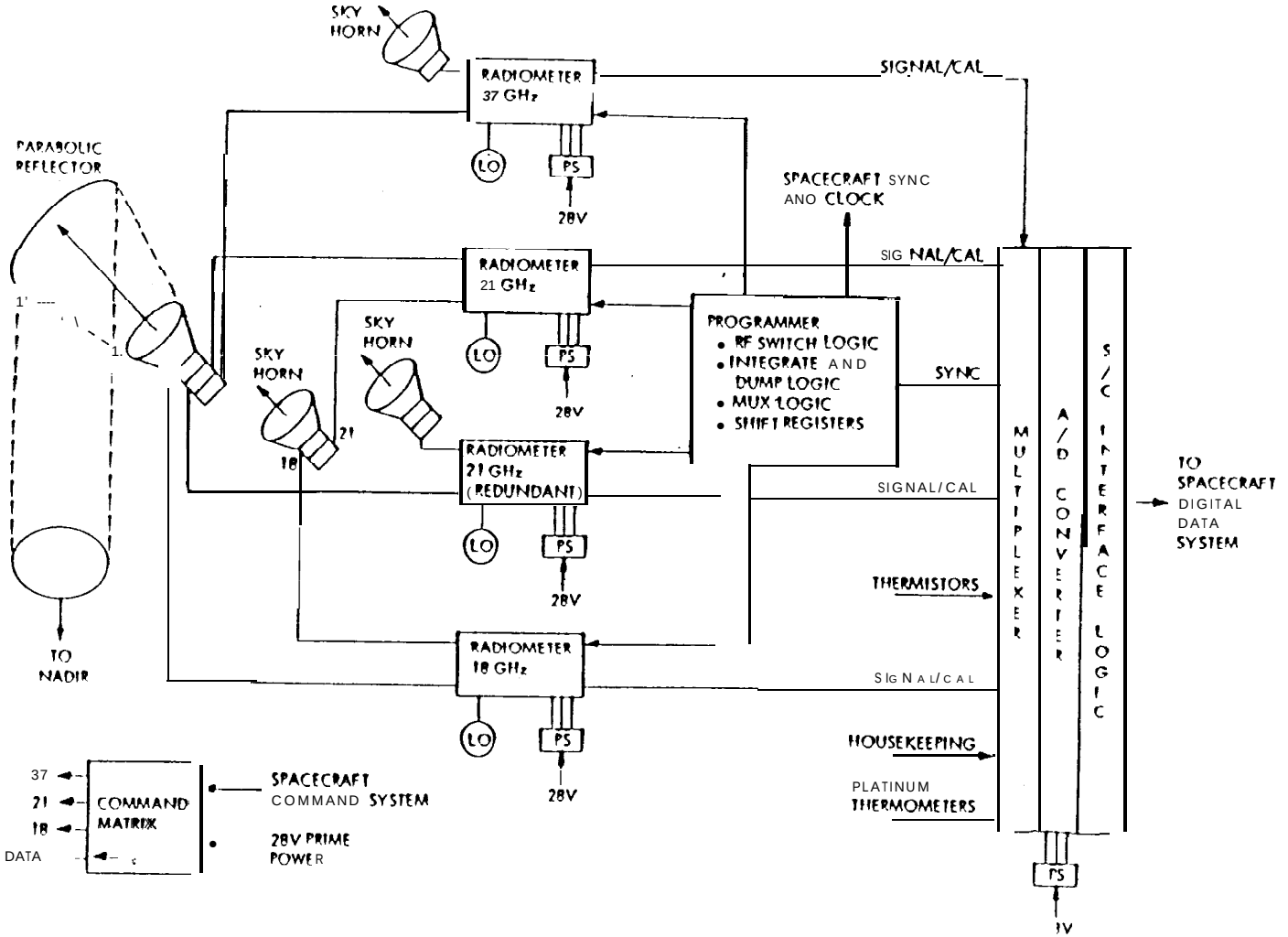

Figure **15.0 The TMR Functional Schematic Diagram illustrates the 4 channel design and connections with the multi-frequency feed horn and the sky calibration horns.**

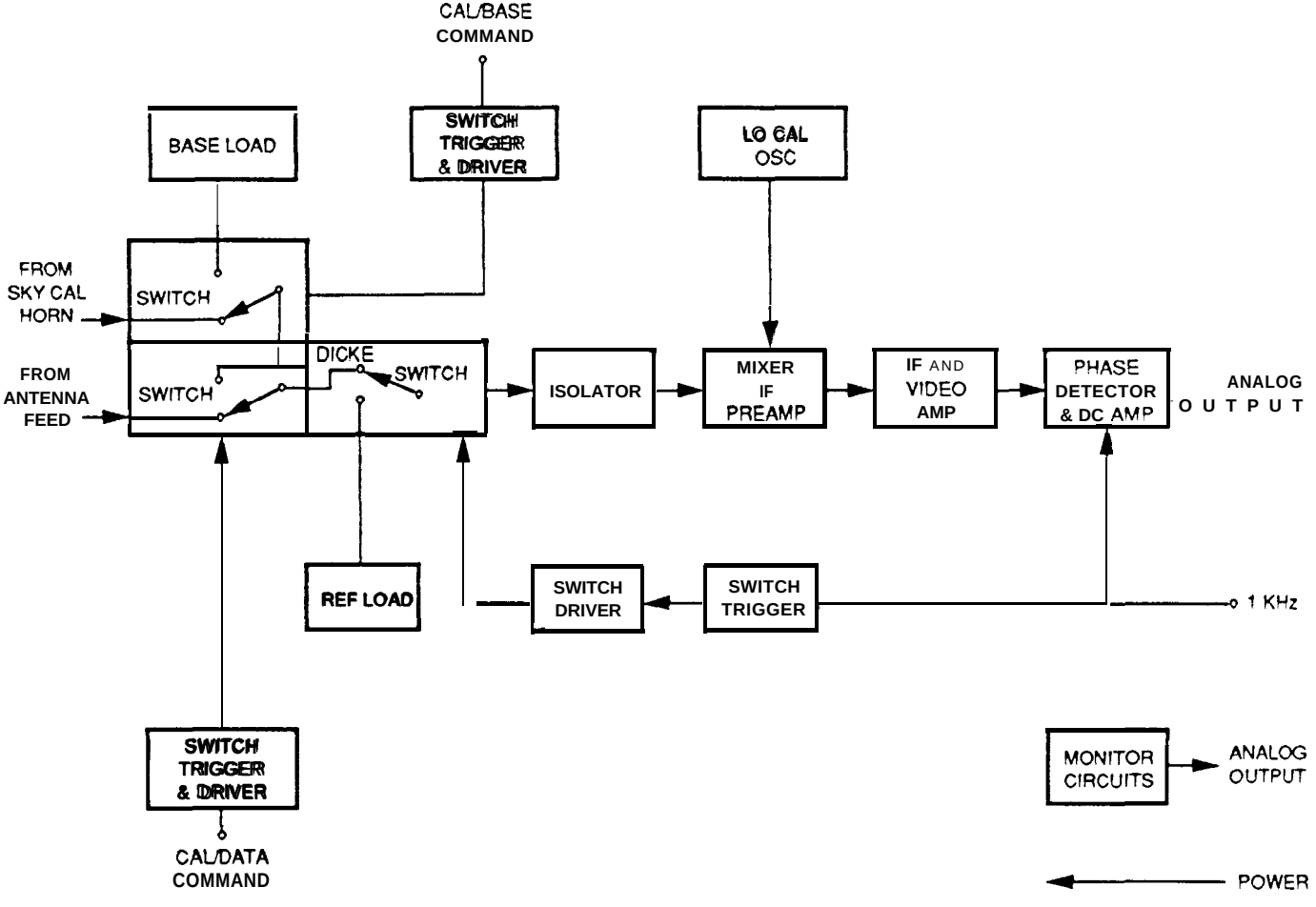

Figure 16.0 Typical **Dicke** switch radiometer channel design used in the TMR.

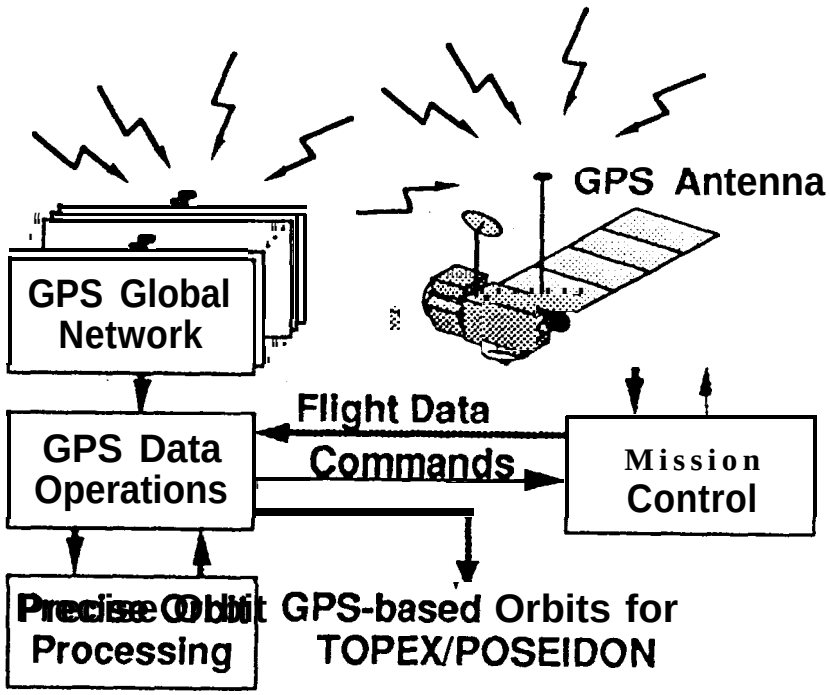

Figure **17.0 The GPS POD system is a global network of GPS satellites, ground based GPS receivers, the satellite flight receiver, and ground operations.**

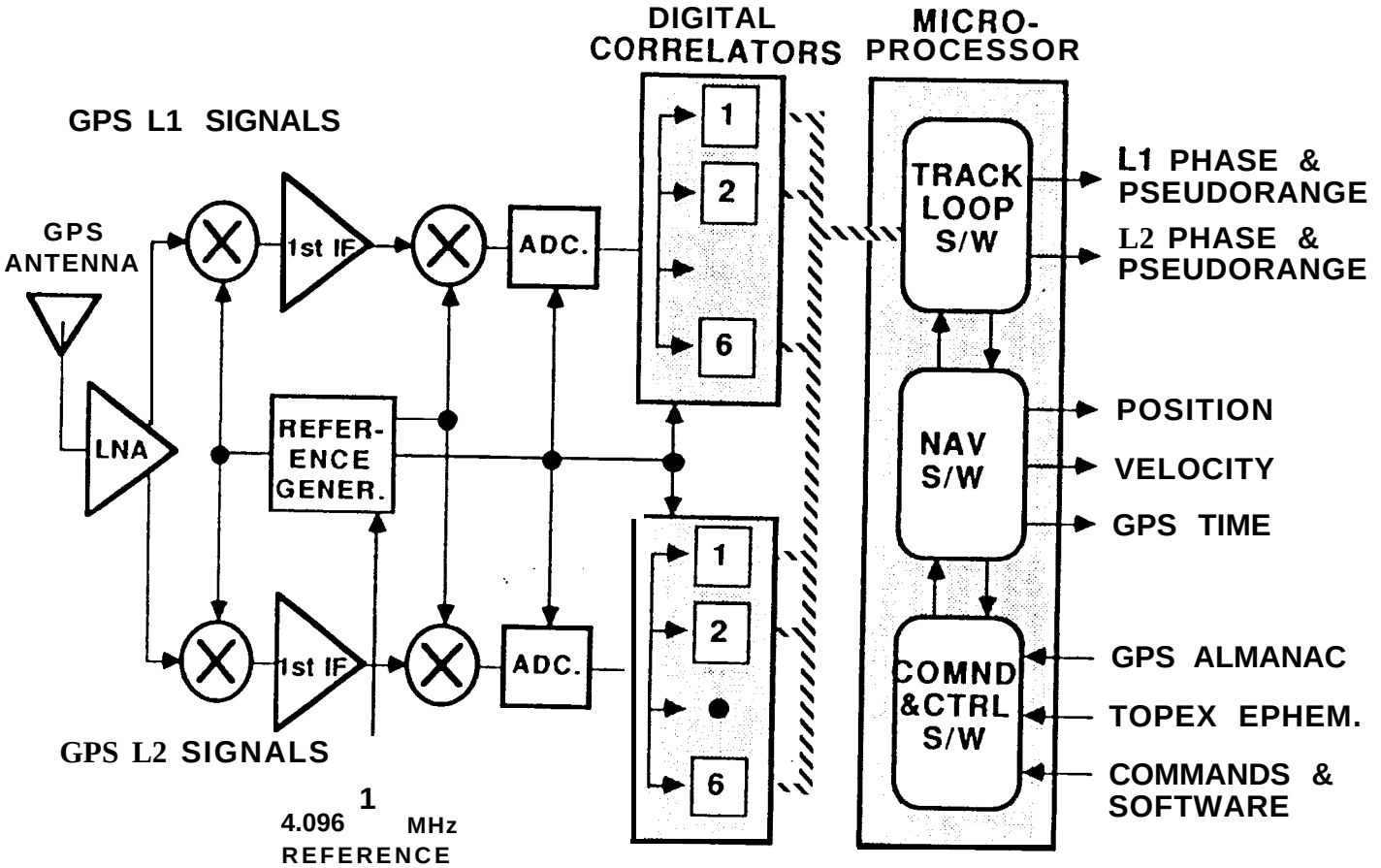

Figure **18.0 The schematic shows the flight system GPS Demonstration Receiver fundamental architecture.**

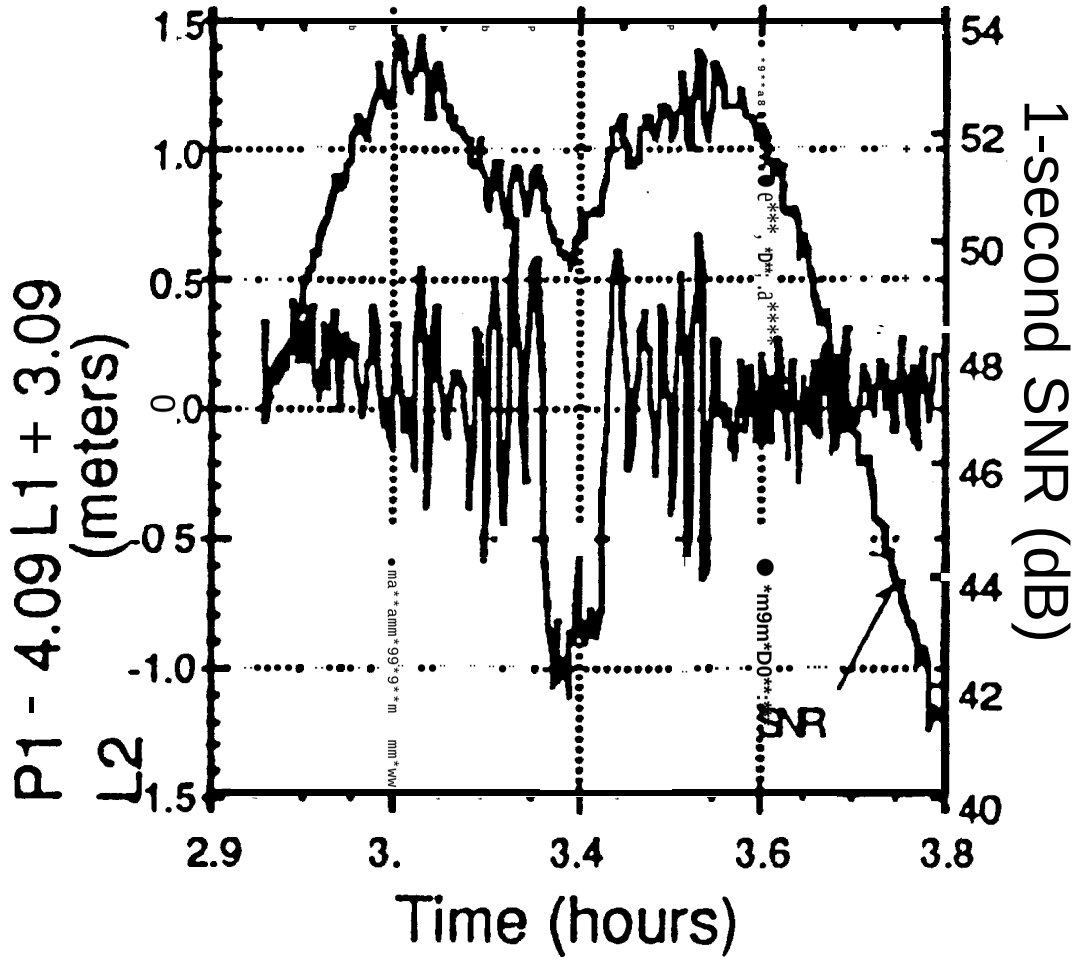

Figure 9.° P1 multipath and SNR taken from flight data are shown vs time. The multipath observable is the linear combination of pseudorange and carrier phase observables which removes the effects of geometry, clocks, and ionosphere, leaving primarily multipath, along with system noise and systematic errors. Ten second normal points are plotted.

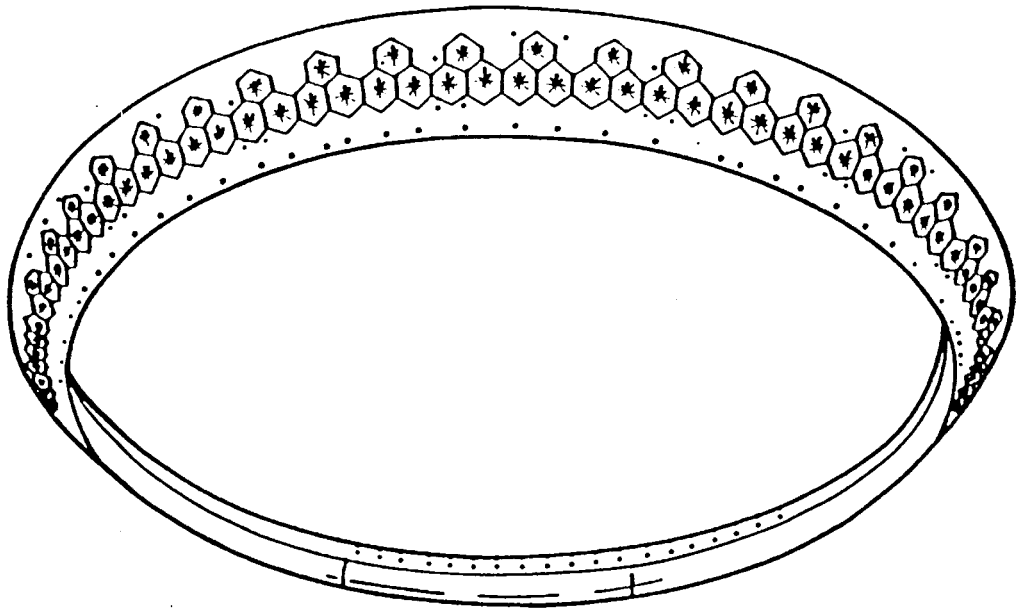

Figure 20 ° LRA as it would appear looking up at the satellite.

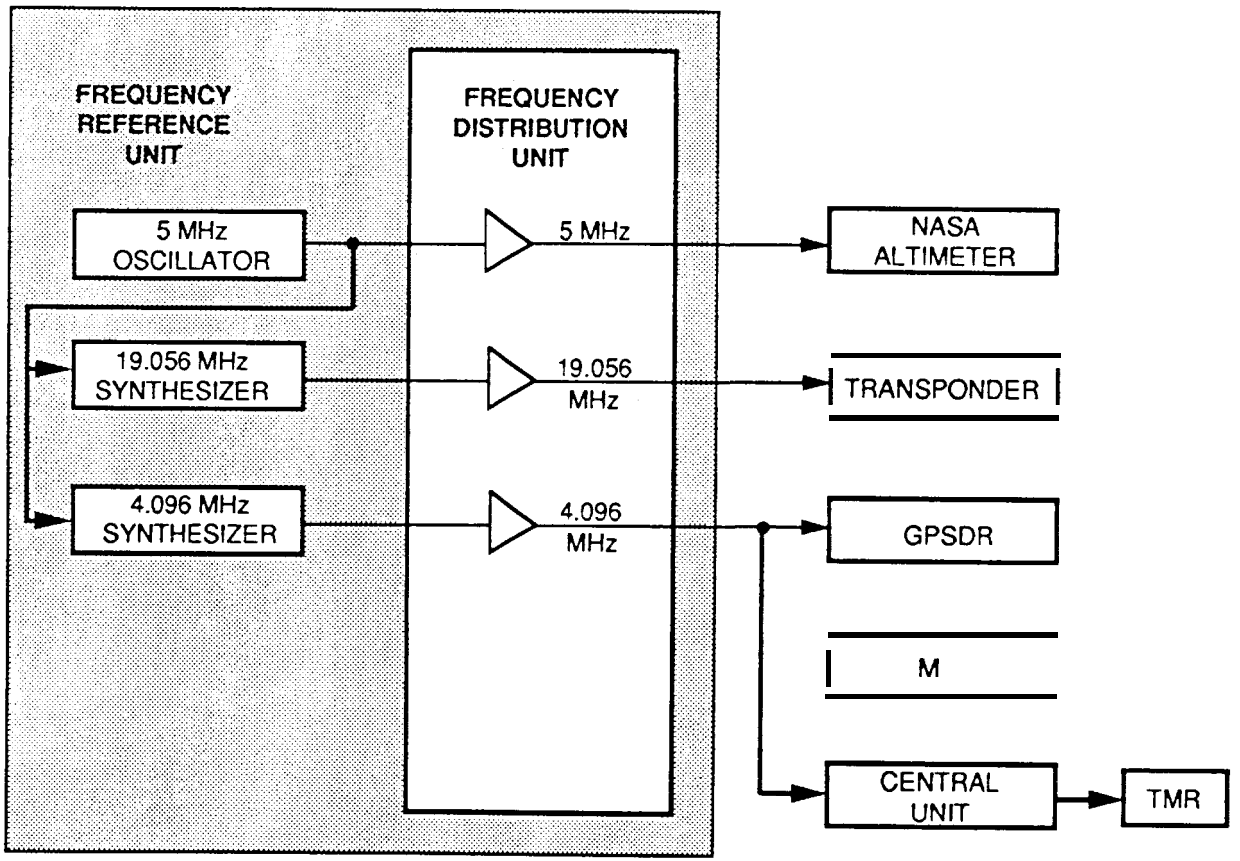

Figure 21.0 The FRU functional diagram and outputs to the NASA altimeter (5 MHz), satellite primary references (4.096 MHz) and satellite transmitter (19.056 MHz).

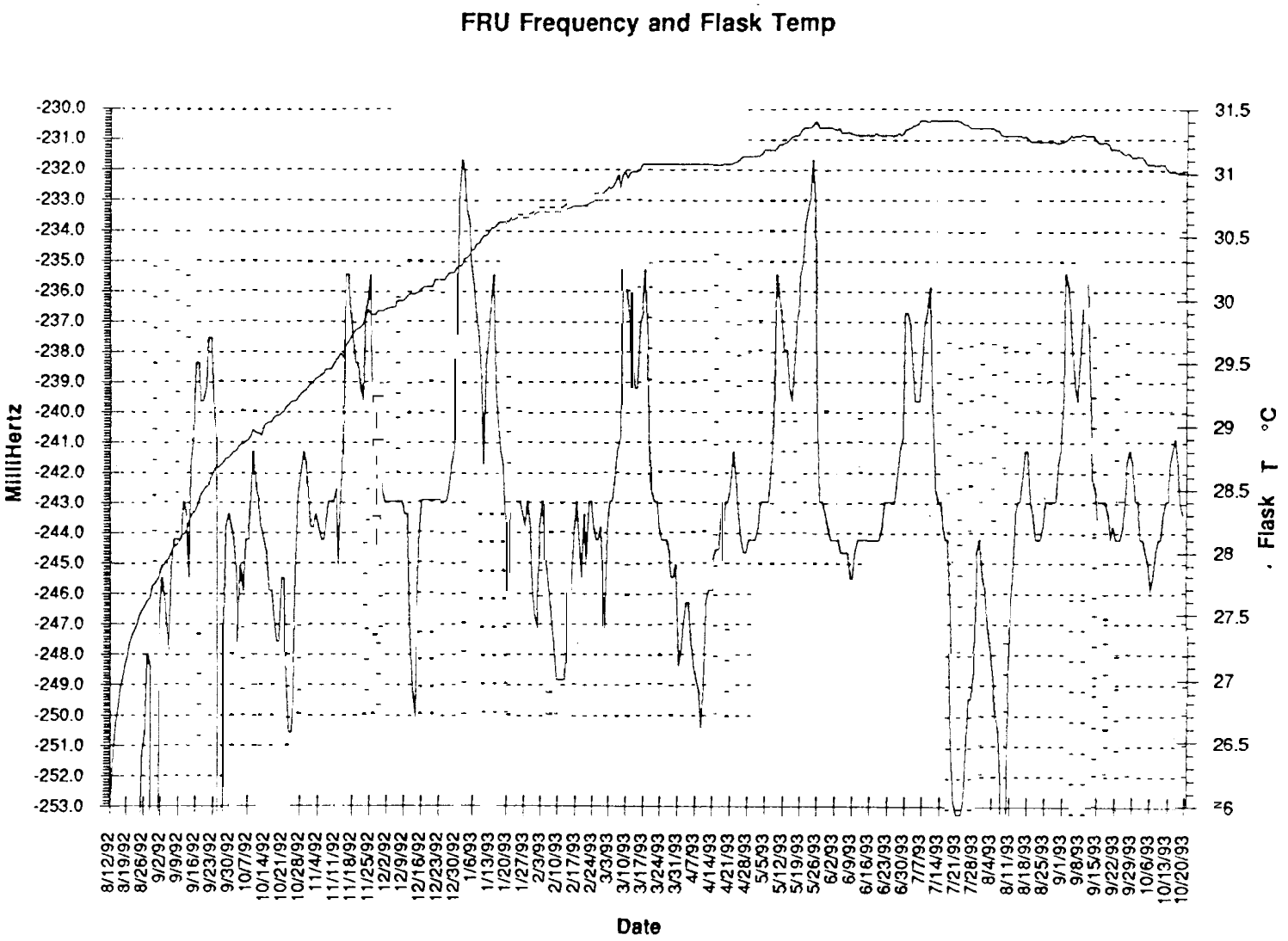

Figure 22.0 The 5.0 MHz Offset in MilliHertz Shown Since Launch

DEFINITIVE GROUND TRACK CHARACTERISTICS

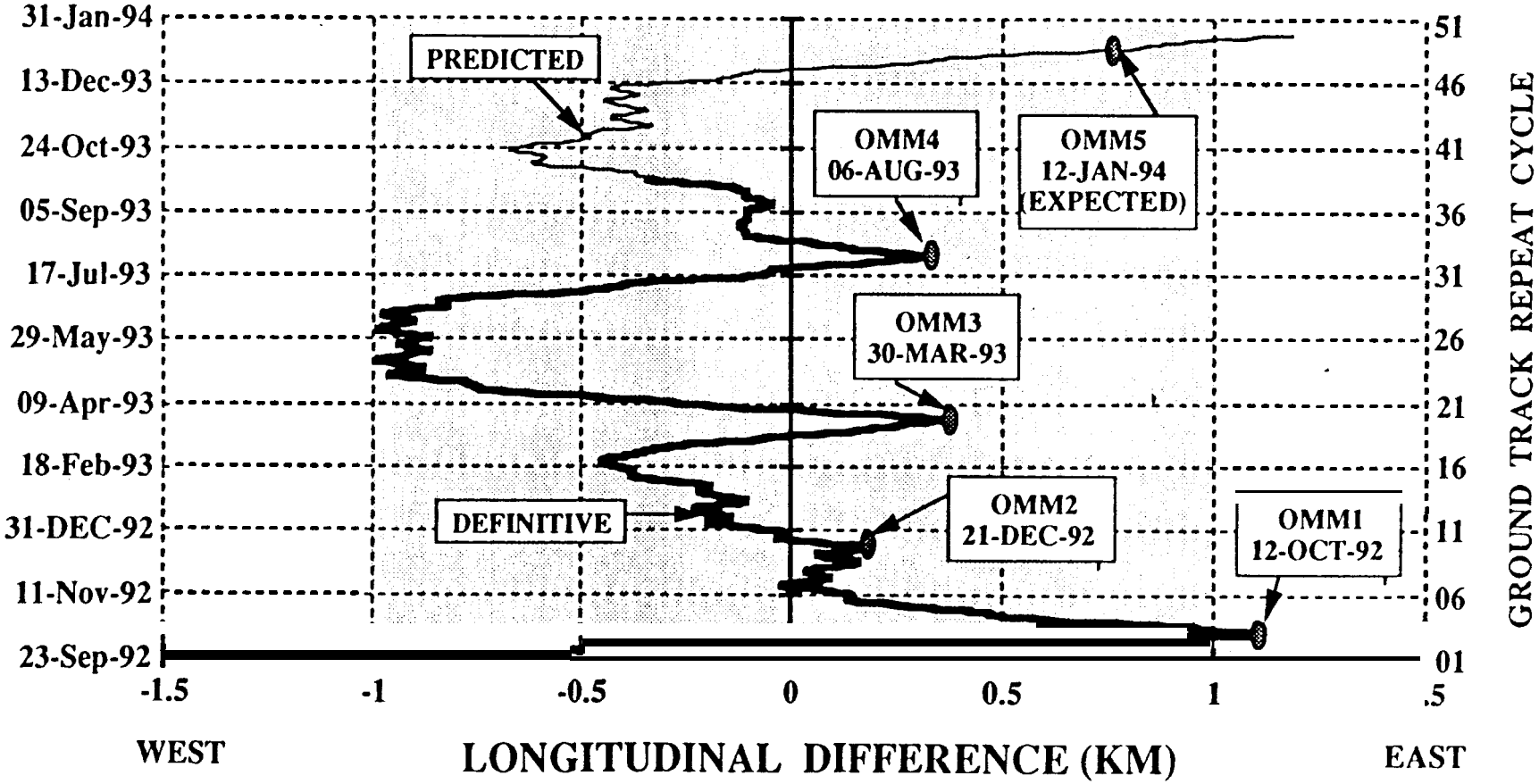

Figure 23.0 The satellite ground track is controlled by performing Orbit Maintenance Maneuvers (OMM) to ta within the ±1 km measurement zone.